Core-shell structure alginate-PLGA/PLLA microparticles as a novel drug delivery system for water soluble drugs

Lim, Ming Pin

2015

Lim, M. P. (2015). Core-shell structure alginate-PLGA/PLLA microparticles as a novel drug delivery system for water soluble drugs. Master’ s thesis, Nanyang Technological University, Singapore.

https://hdl.handle.net/10356/62178

https://doi.org/10.32657/10356/62178

CORE-SHELL STRUCTURED ALGINATE-PLGA/PLLA MICROPARTICLES AS A NOVEL DRUG DELIVERY SYSTEM FOR WATER SOLUBLE DRUGS

LIM MING PIN

2015

NANYANG TECHNOLOGICAL UNIVERSITY

CORE-SHELL STRUCTURED ALGINATE-PLGA/PLLA MICROPARTICLES AS A NOVEL DRUG DELIVERY SYSTEM FOR WATER SOLUBLE DRUGS

LIM MING PIN

SCHOOL OF MATERIALS SCIENCE & ENGINEERING

2015

CORE-SHELL STRUCTURED ALGINATE-PLGA/PLLA MICROPARTICLES AS A NOVEL DRUG DELIVERY SYSTEM FOR WATER SOLUBLE DRUGS

LIM MING PIN

G1200251B

ASSOCIATE PROFESSOR JOACHIM LOO SAY CHYE

SCHOOL OF MATERIALS SCIENCE & ENGINEERING

A thesis submitted to the Nanyang Technological University in partial fulfillment for the requirement for the degree of Master of Engineering

2015

Acknowledgement

First and foremost, I would like to extend gratitude to my supervisor A/P Joachim Loo, for the opportunity given to join the group and to start this project. Without the support and guidance from him, this work will not be at this stage, not the without faith that he had placed in me throughout this period of time.

In addition, thanks to be given to my fellow group members who had provided valuable advice and insight for this project. This includes Dr. Kelsen Bastari, Dr. Charlotte Huang for their experience and problems shared during the work done for this project; Dr Lee Weili, with the advice given during the beginning of the project and also the time spent on advising for the patent and paper manuscript. Not forgetting also Lui Yuan Siang, Sow Wan Ting, and Mustafa Hussain Kathawala for the help given. I would also like to give thanks and credit to my FYP students, Sherwyn Tan, Dickson Tjipto, Kara Cooper, He Xinyan and Leong Wei Wei for their time spent on this project with the hard work they had put in to understand this work in depth further.

Special thanks is given to Dr Effendi Wijaja from Institute of Chemical & Engineering Sciences (A*STAR), for his expertise help with the BTEM / Raman mapping to elucidate the core-shell particulate morphology. Also, my gratitude for the generosity of A/P Phan Anh Tuan, Chung Wan Jun; and Prof Richard Webster from the School of Physical and Mathematical Sciences (NTU) for the use of the Jasco CD spectropolarimeter and the Nicolet Continµum FT-IR microscope. Also, all electron microscopy and X-ray microanalysis performed in this work was conducted in NTU Facility for Analysis, Characterisation, Testing and Simulation (FACTS) laboratory.

I would like to acknowledge and show appreciation for the support given by my colleagues in the MSE Technical Executives group and NTU FACTS Lab, including Dr Goh Chin Foo, Tan Yong Kwang, See-Toh Swee Sing, Nelson Ng, Lim Kian Boon; Dr Tay Yee Yan, Dr Derrick Ang and also the others that I have failed to mention.

I am also grateful to the closer ones who were around during all this time through the more difficult days, especially the cheery folks in MSE Biomaterials Lab (Charlotte, Kelsen, Xuwen and folks; Geok Leng et al, and Siqi; for constantly reminding me that dichotomy can co-exist despite differences – if we wanted to make things happen.

List of Abbreviation

Alg-Polyesteric MP:	Alginate – Polyesteric Microparticles
BCA:	Bi-chronic acid assay
BSA:	Bovine Serum Albumin
CaAlg:	Calcium alginate
DDS:	Drug delivery system
EDX:	Energy dispersive X-ray Spectroscopy
ESE:	Emulsion based solvent evaporation
FT-IR:	Fourier Transform Infra-red
GA:	Glycolic acid
LA:	Lactic acid
LYZ:	Lysozyme
MOI:	Molecule of interest
NaAlg:	Sodium alginate
o/W:	Oil in water (emulsion)
PLGA/DCM:	Solution of PLGA in DCM
PLGA:	Poly (lactide-co-glycolide)
PLLA:	Poly (L-lactide)
PVA:	Poly-vinyl alcohol
SEM:	Scanning Electron Microscopy
w/O/W:	Water in oil in water (emulsion)
w/O:	Water in oil (emulsion)
W_{ext}:	External water phase
W_{int}:	Internal water phase

Table of Contents

List of Figures

List of Tables

Abstract

Recent focus on particle based drug delivery systems, necessitates improved drug loading and sustainable release for water soluble drugs. Biodegradable polyesters, such as poly (lactide-co-glycolide) (PLGA) and poly (L-lactide) (PLLA), are well studied but are insufficient in terms of encapsulation efficiency for water soluble drugs and providing a stable environment for macromolecule encapsulation. Even though hydrogels could allow for higher encapsulation efficiency of water soluble drugs, they are inadequate in terms of sustained and controlled release. Hence, the aim of this study was to develop a particulate drug delivery system, with drug-loaded alginate hydrogel core, encapsulated by a hydrophobic polyester shell. This is hoped that this would improve the loading of water soluble drugs, while allowing for the release behavior to be governed by the core-shell geometry of the particulates formed. In addition, the hydrogel core is also expected to perform as a stable and friendly environment for protein encapsulation.

In this work, a one-step fabrication method of core-shell microparticles by concurrent ionotropic gelation and solvent extraction was studied. The resultant microparticles fabricated, have a core-shell structure of calcium alginate, encapsulated in a shell constructed of either PLGA or PLLA. The cross-sectional morphology of particles was established via scanning electron microscopy, Raman mapping and selective dissolution of hydrogel material. The incorporation of alginate within the microparticles was shown to improve loading efficiency of model hydrophilic drug metoclopramide (MCA). Release studies also showed that the polyesteric shell functioned as a limiting barrier in drug release from a MCA loaded drug hydrogel core. Lysozyme and bovine serum

albumin released from the microparticles fabricated, show similar behavior in release controlled by the polymeric shell, and also the preservation of bioactivity and protein structure post release.

It is also noted that the double emulsion based fabrication method, relies on concurrent ionotropic gelation of the alginate dissolved within the internal aqueous phase of the double emulsion to form calcium alginate; and solvent evaporation to cause precipitation of the shell polymer. It is also put forward that the oil layer of the double emulsion, consisting of a hydrophobic polymer dissolved within a volatile solvent during fabrication, act as a semi-permeable membrane during fabrication and is subject to osmotic pressure forces acting from both aqueous phases. The permeability of this oil layer, the solvent extraction and polymer precipitation rate; effects of osmotic pressure; double emulsion stability; affects the particulate fabrication in terms of the cross sectional morphology, surface morphology and also subsequently release behavior.

Hence, it is hoped that this new particulate drug delivery system would be valuable in areas such as delivery of macromolecules, including peptides, proteins and vaccine antigens. Consequently, these hydrogel-core hydrophobic polymer-shell microparticles would permit the improved encapsulation and release of water soluble drugs, and provide a safe environment for loading bioactive molecules.

Chapter 1 Introduction

1.1 Background

Drug delivery systems for pharmaceutical drug administration, are studied for controllable release of therapeutic drugs, to improve efficiency of treatment regimen and patience compliance for disease management [1, 2].

In particular, water soluble drugs including antibiotics, anti-cancer drugs, growth factors and vaccines antigens, were of increased interest [3, 4]. Particulate drug delivery systems incorporating FDA approved biodegradable polymers such as PLGA and PLLA, are well studied for their capability for sustained release [5]. However, shortcomings of the use of such polymers include reduced loading efficiencies of water soluble drugs due to their hydrophobic nature [3]. This reduced loading is also attributed to the fabrication methods used, when drugs are leached to the external water phase during the use of emulsion based solvent evaporation techniques [6].

In addition, the stability of proteins encapsulated in polyesters is known to be an issue, due to interactions between the polymer matrix and the encapsulated macromolecules during fabrication and release [7]. Hydrogels on the other hand, such as alginate and chitosan were explored for better encapsulation of water soluble drugs [8] and a friendly environment for protein encapsulation [9]. Hydrogels are however insufficient in terms of sustainable release, due to their susceptibility to swell when immersed in an aqueous medium as result of the gel high porosity [10].

1.2 Problem statement

Given the issues and limitations attributed to both PLGA and hydrogel based drug delivery systems, a particulate drug delivery system incorporating a drug loaded gel core within a PLGA shell is sought after. Examples of such composite polymeric systems are already reported in literature [11-13], where PLGA microparticles are fabricated with gel material dispersed within [12], or on PLGA microparticle surfaces [11]. However, the hydrogel material used in these methods has to be pre-fabricated in an extra step, requiring further effort and time during microparticle fabrication. In addition, protein stability and bioactivity is known to be an issue during fabrication, storage and release; due to the acidic microclimate of these polyesters [14].

1.3 Objectives

The objectives of this study are as follows:

1. Develop a single-step method to produce core-shell alginate-polyester microparticles (Alg-Polyesteric MP) for the purpose of encapsulation and release of water soluble drugs, and also to explore the mechanism of particulate formation.
2. Characterize and study the above mentioned particles on the drug loading capacity, and release behavior using a low molecular weight water soluble drug.
3. Characterize and study particles fabricated using the above mentioned method, loaded with model proteins, including the drug loading capacity, release behavior, protein structure and bioactivity post encapsulation and release.

1.4 Novelty

The aim of this study is to fabricate a particulate system incorporating a hydrogel-core/hydrophobic polymer-shell within a single step. It is theorized that this would increase the encapsulation efficiencies for water soluble drugs to be used in a PLGA/PLLA based controlled drug delivery vehicle; and at the same time allow for a controlled release behavior governed by the core-shell geometry of the particulates formed.

In addition, by fabricating microparticles with proteins encapsulated in the above manner, it is hoped that this will assist in preserving the bioactivity of proteins, with the presence of a hydrogel component to house the protein molecules within the hydrogel.

1.5 Scope

The scope of the work reported covers the fabrication technique of microparticles with variations of the shell polymer constructed, which include alginate-PLGA microparticles (Alg-PLGA MP) and alginate-PLLA microparticles (Alg-PLLA MP). Metoclopramide HCl (MCA) as a model hydrophilic was loaded in the above mentioned particles, to examine the loading capacity and release behavior. Parameter variations for particle fabrication examined in this study, include the emulsification power of the primary emulsion, and also volume of the external water phase.

Model proteins, lysozyme and bovine serum albumin (BSA), were also loaded in microparticles fabricated using the above technique. Besides the release behaviour and

the particulate morphology, the structure of released BSA was also characterised using SDS-PAGE and circular dichronism. The Micrococcus lysodeikticus lysing assay was used to determine the lysing activity of lysozyme post-release. Parameters variations include the change of cross-linking ion concentration in the external water phase, and the volume of external water phase; to examine their effects on the microparticles formed and their drug release behaviour.

Chapter 2 Literature Review

2.1 Drug delivery systems

Drug delivery systems (DDS) are used to provide an alternative means of pharmaceutical drug administration, by acting as a storage vehicle that can be introduced to the body to provide controlled release of the encapsulated payload while maintaining the required therapeutic concentration levels and reducing the systemic burden for some treatment regimens, as a result of systemic distribution of the drugs required [15].

Some of the different form factors of these systems include implantable material such as casted films, slabs or particulates. These systems are delivered into the body via different administration routes, including enteral, transdermal, oral, intravenous or intramuscular injection routes [16]. When these DDS are introduced into the body, they can become localized depots for release of pharmaceutical drugs near the targeted area of delivery, instead of systemic distribution of therapeutics taken by other routes [17]. Such pharmaceutical drugs include small molecules such as isoniazid, gentamicin and ofloxacin for antibiotics; macromolecules proteins such as, growth factors, antigens, viral, etc. [4]. Examples of DDS systems currently in commercial use includes Lupron, Somatulin and Ozurdex [18].

Materials used for drug delivery systems, span across various classes of biocompatible materials, including polymers such as synthetic polyorthoesters, poloaxmers, polyphosphazenes and natural polymers such as alginates and chitosan [19]. Other materials include inorganic materials such as hydroxyapatite and silica dioxide [20, 21].

Among the different materials used, poly(lactide-co-glycolide) and poly(L-lactide) are among the most researched in-depth [5]. These polyesters are biodegradable and capable of encapsulating molecules for controlled release. They are however insufficient when it comes to water soluble drugs, due to the polymer's hydrophobicity and its resultant deleterious effects on the bioactivity of loaded proteins [4, 7]. Hydrogels such as calcium alginate or Poly-(N-isopropylacrylamide) on the other hand, encapsulate drugs within a porous network, but are prone to burst release due to their porous nature and their propensity to swell in release medium [10].

2.2 Materials background

2.2.1 Biodegradable polyesters

Poly-(lactide-co-glycolide) (PLGA) and poly-(L-lactide) (PLLA) are a category of polyesters well researched for their biocompatibility, biodegradability, and their capacity to allow for sustained release of encapsulated molecules of interest [5, 22]. Essentially, PLGA and PLLA are made up of monomer units of lactide (LA) and glycolide (GA) connected via ester linkages, as shown in **Figure 2.1**:

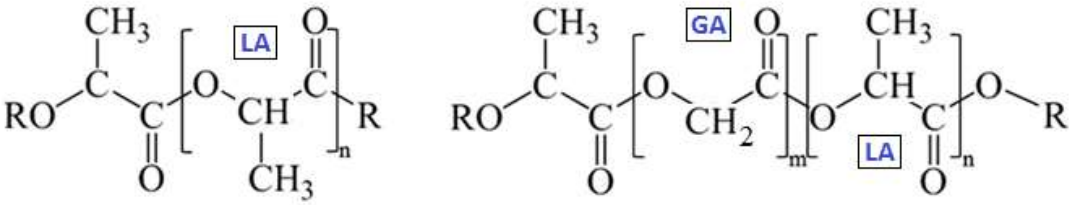

Figure 2.1: Structure of the PLGA and PLLA, indicating the respective LA and GA monomers. [23]

PLGA and PLLA are already extensively studied and are in fact employed in commercial applications such as Lupron Depot for the treatment of prostate cancer [24]. These polymers degrade via hydrolysis and releases any encapsulated therapeutics from within the polymer matrix. The release of encapsulated drugs is variable via the rate of diffusion through the polymer matrix and also the degradation process occurring within or on the surface of the polymer matrix. PLGA for example, is known to have release rates dependent on the hydration of the polymer matrix when immersed within a release medium; due to the different degradation states of the polymer, with varying levels of chain scission, the dissolution of oligomers; and complete dissolution of the polymer matrix [25, 26].

The LA:GA ratio in the co-polymer PLGA or PLLA, dictates the different physiochemical and release behavior of the polymers. For example, PLLA has a higher lactide content compared to PLGA and hence is more hydrophobic due to the additional methyl groups found on the lactide monomer. Hence, PLLA is known to degrade slower than PLGA through hydrolysis due to a decreased water intake. PLGA synthesized with different LA:GA ratios will hence degrade at a different rate as a result. Since the difference in degradation behavior due to differing LA:GA content affects the release behavior of drugs encapsulated (as seen in **Figure 2.2**, for different types of PLGA), this can allow for customizable drug release rates in this context. In addition, the different molecular weight of polymer used, will also affect the degradation rate and subsequently the release rate of encapsulated molecules. [27, 28] .

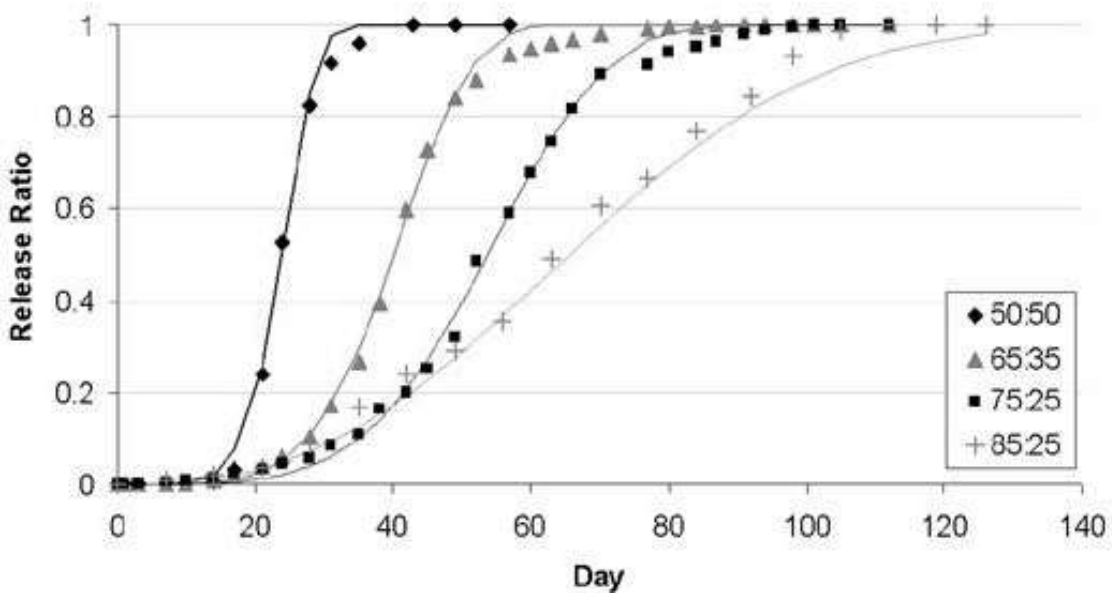

Figure 2.2: Drug release behaviour between the different LA:GA ratio of PLGA [27]

Fabrication techniques of polymeric particulate DDS are extensively studied, which involve methods of emulsion solvent evaporation, nanoprecipitation, and coacervation [27, 29]. However, some of the issues encountered when using the above mentioned techniques, include reduced loading efficiencies of water soluble drugs, due to the hydrophobic nature of the polymer used [3]. This reduced loading is also attributed to the fabrication method, when drugs are leached to the external water phase during the use of emulsion based solvent evaporation techniques [6].

In addition, the stability of proteins encapsulated is known to be an issue, as a result of interactions between the polymer matrix and the encapsulated macromolecules [4, 7]. This becomes a problem during the release of proteins, in addition to the deleterious effect of common fabrication methods, which involve the use of organic solvents. Burst release from PLGA particulate DDS is also an issue, as a result of localization of drugs on

particulate surfaces and within the pores formed in the matrix of microparticles [4, 5, 7, 30].

2.2.2 Alginates

Alginates are a class of natural biopolymers sourced from brown algae and bacteria. A type of anionic polysaccharide, it is a co-polymer consisting of manuronic acid (M) and gluronic acid (G) units that make up the entire polymer chain.

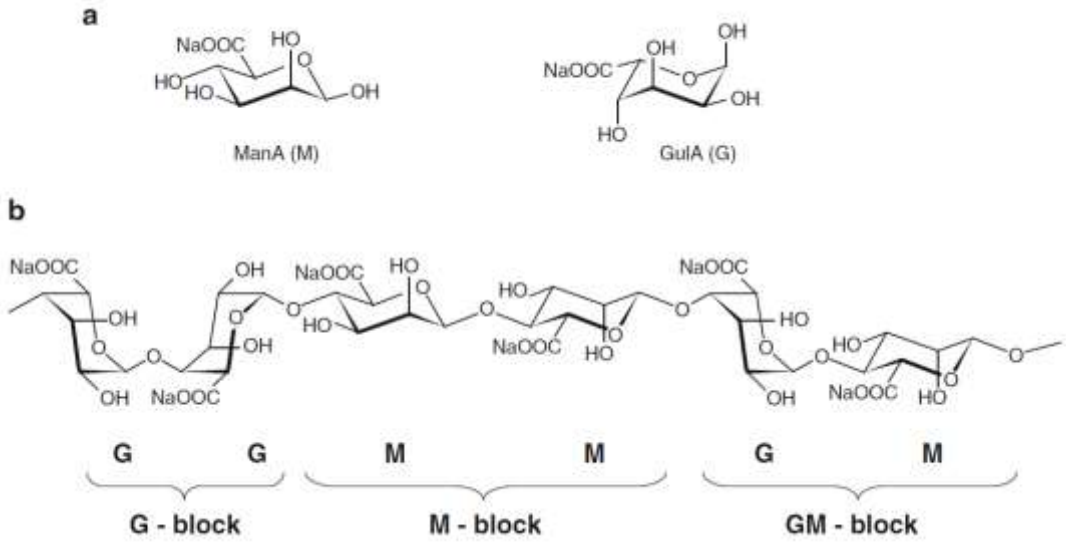

Figure 2.3: (a) Monomer units of alginate; manuronic acid (M) and gluronic acid (G) (b) the three different possible block compositions of the alginate co-polymer [31]

The uronic acid units are linked by glycosidic bonds and are arranged in blocks of MM, MG, or GG units, as shown in **Figure 2.3**. The composition and sequencing of M and G units is variable among different sources of algae, giving rise to different viscosity ranges of alginates available for use. The sodium salt of alginate (NaAlg) is also water soluble [31-34].

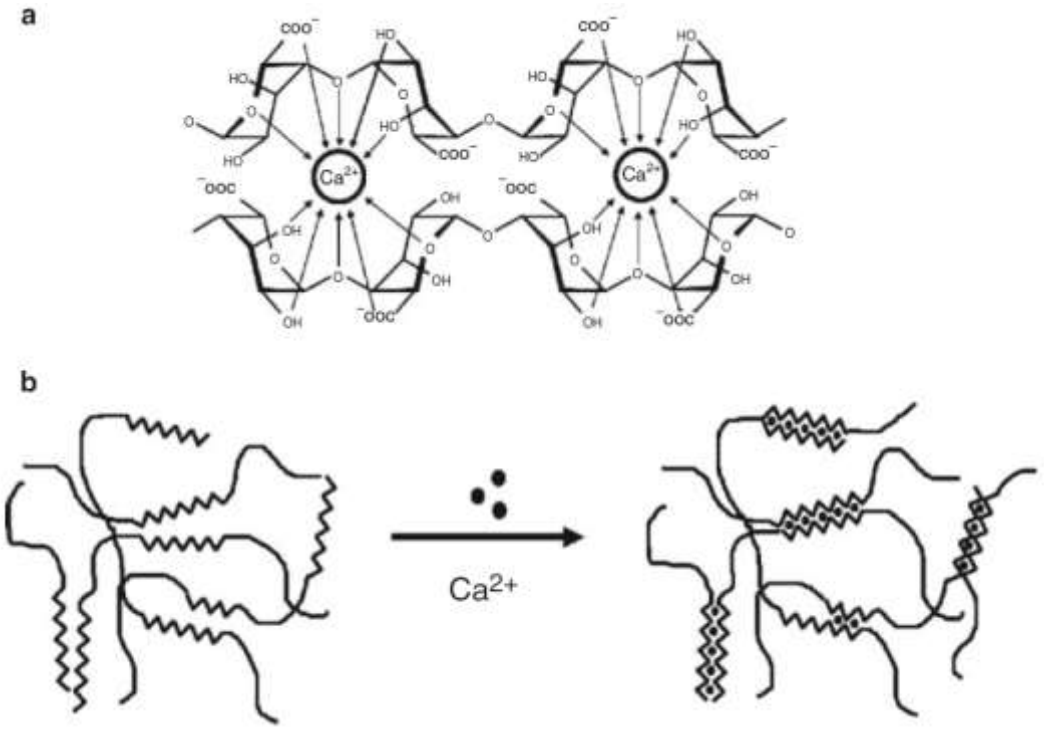

Figure 2.4: (a) Egg box model; (b) illustration of gel formation with the creation of inter-chain junction zones. [31]

Alginates can be physically gelled together with divalent ions, including Ca^{2+}, Mg^{2+}, Ba^{2+}, etc. This results in an "egg box" structure, where uronate units of the copolymer are bound strongly by Ca^{2+} ions through chelation based binding, forming physical cross-links i.e. junction zones [31]. With the combined formation of various types of junction zones (shown in **Figure 2.4b**), this results in the formation of an ionotropic gel that is insoluble in water. Hence, the gel is usually formed by dripping or casting into a $CaCl_2$ bath. Disruption or dissolution of this gel requires the presence of sequestering agents like citrate, EDTA, phosphate buffer saline to remove the Ca^{2+} ions from the junction zones [34].

Alginates are actively studied in pharmaceutical and medical settings, such as for drug delivery, cell encapsulation, wound healing, and tissue engineering applications [10, 33, 35]. With regards to drug delivery however, it is limited in terms of sustained release of low molecular weight drugs due to the propensity of hydrogels to swell in water, as a result of its porosity when immersed in an aqueous environment [10, 35].

2.2.3 Encapsulated molecules of interest

2.2.3.1 Metoclopramide hydrochloride

Metoclopramide hydrochloride (MCA) is a low molecular weight drug (336.26 Da), which is water soluble and is used as a model drug in this study. MCA is a gastroprokinetic drug prescribed for gastric stasis and nausea [36]. It is also reported to function as a radio-sensitizer and chemo-sensitizer for lung carcinoma treatment [37, 38]. MCA can be detected via UV-Visible spectroscopy with an absorbance of 309 nm, and also demonstrates a detectable fluorescence emission at 360 nm when excited at 310 nm. [39]

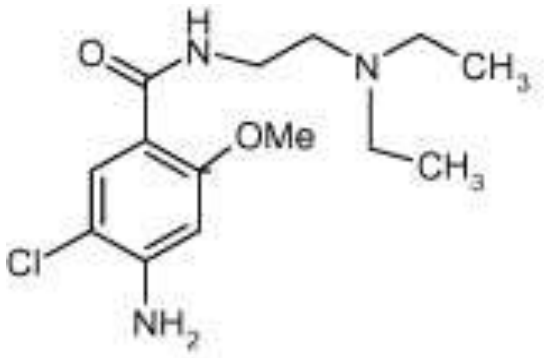

Figure 2.4: Molecular structure of metoclopramide HCl [38]

2.2.3.2 Lysozyme

Lysozyme, i.e. N-acetylmuramichydrolase or muramidase, is a small molecular weight protein (14.4 KDa) [40], found naturally in tears, egg white and milk [41]. Being an antimicrobial enzyme, it is effective against gram-positive bacteria via its lysis action against the peptidoglycan cell wall [42]. The cleavage of glycosidic linkages between N-acetylmuramic acid (NAM) and N-acetylglucosamine (NAG) in peptidoglycan cell wall of bacteria by lysozyme (**Figure 2.5**), can be used to determine the activity of lysozyme by monitoring the turbidity change in a *Micrococcus lysodeikticus* lysing assay [43].

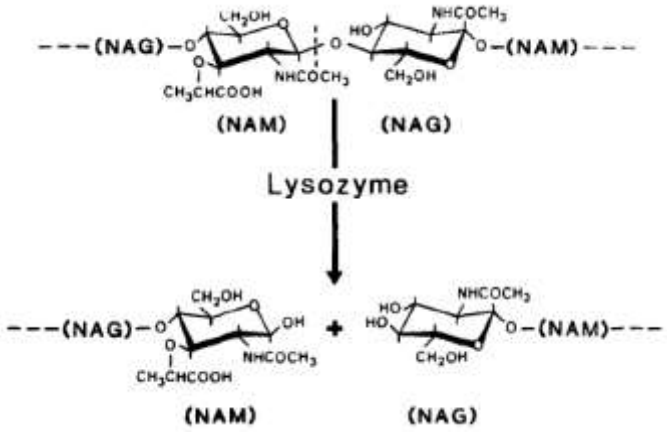

Figure 2.5: Lysis of peptidoglycan cell wall (backbone polymer of NAG and NAM) with lysozyme

2.2.3.3 Bovine serum albumin

Bovine serum albumin (BSA) is a globular protein (66.4 KDa) obtained from bovine blood, commonly used as a model protein for studies, due to its availability from livestock as compared to human blood. Like all mammalian serum albumin, BSA provides oncotic pressure and is a carrier for molecules such as fatty acids or hormones in blood [44-46]. BSA is also known as Fraction V, obtained via the Cohn process initially planned for use as a blood expander in medical use during the 1940s [47]. Structural-

wise, BSA consists of 54% α-helix & 14% β-helix domains [48]. BSA is used in a variety of lab applications, for e.g. as a blocking agent in immunoassays such as enzyme-linked immunosorbent assays (ELIZA) and western blots [49, 50]; and as a protein concentration standard in quantification assays [51, 52].

2.3 Fabrication methods

2.3.1 Fabrication of polyesteric microparticles

Microencapsulation of drugs within PLGA or PLLA, usually involves dissolving the polymer in an organic solvent, together with the molecule of interest (MOI), and then subsequently casted into the form factor required. For microparticle fabrication, casting methods include emulsion based solvent evaporation/extraction methods, coacervation (phase separation) and spray drying, nanoprecipitation (**Figure 2.6**) [4, 5, 29]. Among these methods, the emulsion based solvent evaporation (ESE) method is the most commonly studied [6, 53, 54].

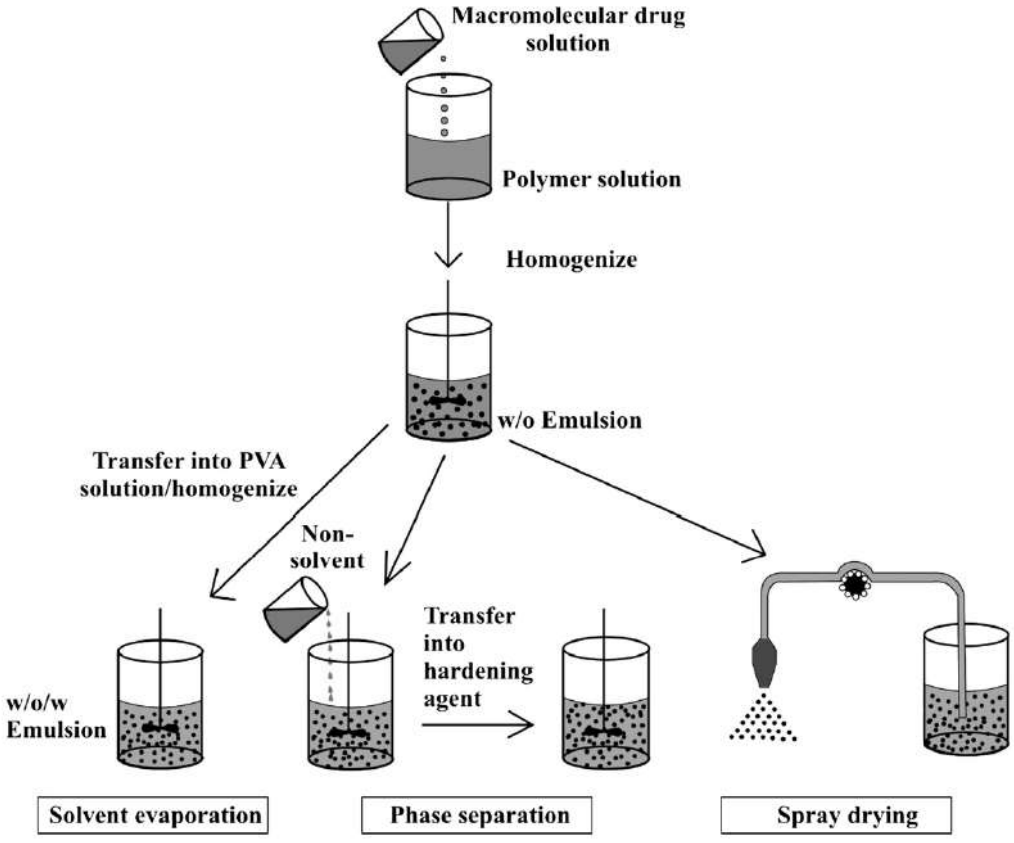

Figure 2.6: Scheme depicting the various methods of particulate fabrication [4]

A typical ESE method is depicted in **Figure 2.7** and described as follows:

1. A drug molecule of interest (MOI) is dissolved or suspended within a PLGA polymer solution. The PLGA solution is typically consisting of PLGA dissolved in a volatile solvent, such as ethylene chloride or ethyl acetate.
2. The PLGA solution is subsequently dispersed into an external water phase with poly-vinyl alcohol (PVA) surfactant to form an oil-in-water (o/W) emulsion.
3. As the organic solvent making up the PLGA solution is extracted or evaporated during the emulsification, the hardened microparticles with the encapsulated MOI are left in the external water (W_{ext}) phase and collected for further processing. [2].

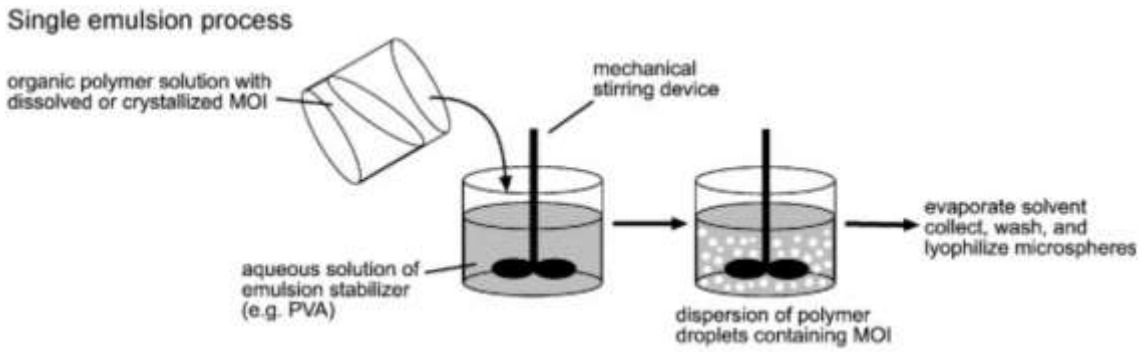

Figure 2.7: Illustration of an o/W emulsion solvent evaporation process [2]

In the ESE method of particulate fabrication, the emulsion formation serves to template the spherical shape of microparticles formed, via the formation of emulsion droplets. The hardening of the emulsion droplets into microparticles and precipitation of polymer, is reliant on the extraction of solvent from the emulsion droplets into the W_{ext} phase before evaporation into the atmosphere [6].

Due to the hydrophobic nature of the polymers used, water soluble drugs are more commonly encapsulated using a water-oil-water (w/O/W) double emulsion instead. In this case, the water soluble drug is dissolved within an internal water (W_{int}) phase, before later dispersion into a PLGA solution, forming water-in-oil (w/O) emulsion as the first step. The primary w/O emulsion is then subsequently dispersed into a W_{ext} phase, as depicted in **Figure 2.8** to form a w/O/W emulsion [2, 53].

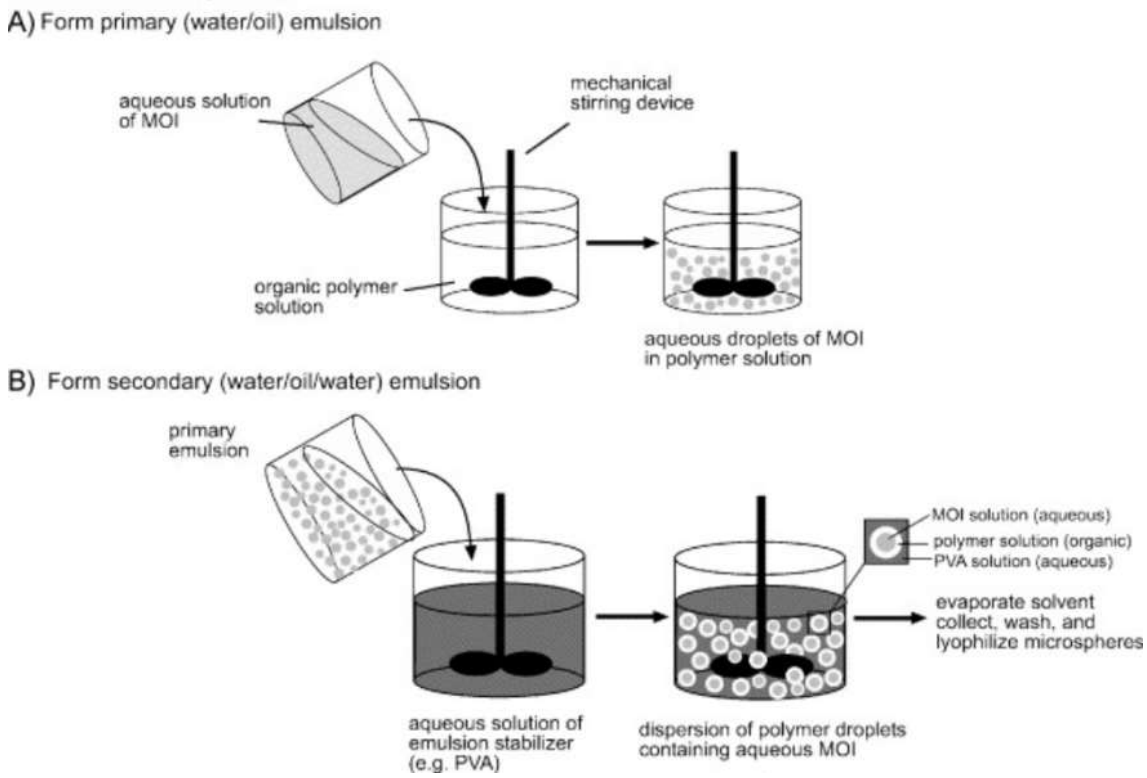

Figure 2.8: Illustration of a w/O/W double emulsion solvent evaporation process [2]

As the main process of particulate formation involves the forming a double emulsion and subsequent emulsion droplet hardening via solvent extraction, factors affect the encapsulation efficiency of the particles formed, are as follows:

- Solubility of encapsulated MOI when compared to W_{ext} phase: water soluble drugs usually leaches out to the external water phase in a w/O/W double emulsion, due to the drug's hydrophillicity, reducing the encapsulation efficiency [30].

- Solvent extraction rate: the solvent extraction rate is proportional to the rate of polymer precipitation and solidification of the emulsion droplets. The encapsulation efficiency is reported to improve with a fast extraction rate, due to reduced time for MOI to leach out to the W_{ext}. The solvent extraction rate is also controllable by amount of external water phase used, varying the rate of solvent partitioning into the external water phase before evaporation [30, 55].

- Stability of double emulsion: double emulsions are known to be inherently unstable and the inner water phase has a tendency to coalesce with the external water phase over time [56]. This results in loss of MOI and reduced encapsulation efficiency as a result.

  Emulsion stability can be improved with the use of surfactants such as Span80 or Tween80. An increase of viscosity of either of the phases also increases the emulsion stability, e.g. increase in polymer solution concentration or molecular weight of the polymers used [30, 57, 58].

- Osmotic pressure between aqueous phases and oil phase: due to the presence of solute dissolved within the internal and external aqueous phases, the oil layer (i.e. polymeric solvent layer) of the double emulsion behaves like a semi-permeable membrane prior

to hardening. As a result, the double emulsion can exhibit the effects of hypotonicity or hypertonicity, dependent on the solutes dissolved in the aqueous phases [58].

Hence, a reduction in an osmotic gradient as direct result of solutes dissolved in the aqueous phases can reduce formation of water channels or rupture of double emulsion droplets formed, improving encapsulation efficiency. In addition, care taken on the direction of the osmotic gradient may reduce out flux of MOI to the external phase [30, 58].

Pertaining to protein encapsulation, **Figure 2.9** below shows the typical steps in the ESE fabrication process and the various factors that would affect release, especially macromolecules:

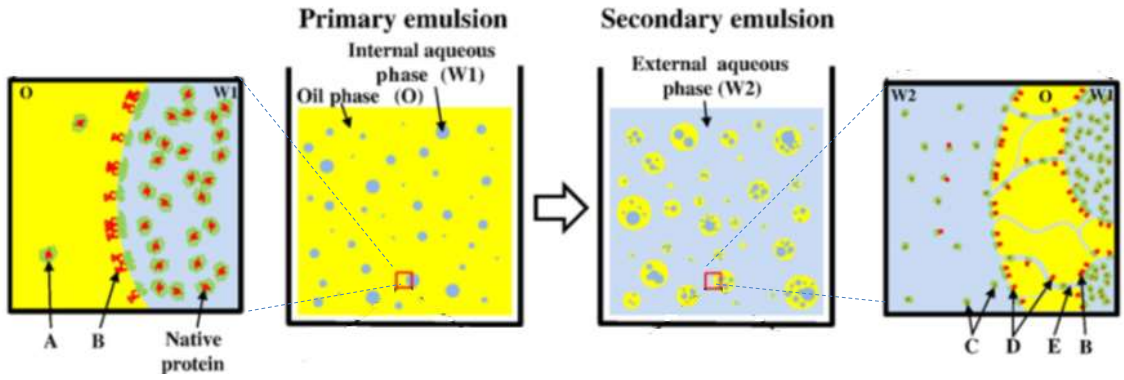

Figure 2.9: The different stages in ESE fabrication and the different deleterious effects on protein release; inset shows a close up on the emulsion phase interfaces [7]

- A, B: Partitioning of proteins into organic solvent used, and the water-solvent interface can cause denaturation of protein due to the amphiphilic nature of proteins.

- D, E: With the forming of a w/O double emulsion droplet, water channels formed in the oil/solvent phase would allow proteins to move from the inner to external phase, resulting in increased exposure of water/oil interfaces and chances of protein deactivation and also reduction of encapsulation efficiency.

- E: The water channels formed will become pores and channels for encapsulated MOI to leach out during release, causing burst release. [7]

2.3.2 Fabrication of alginate hydrogel

To fabricate alginate hydrogel particulates or beads, the alginate is dissolved in water and then exposed to the divalent ions required to cause physical cross-linking i.e. gelation. Gelation of alginates can either occur via diffusion setting or internal gelation:

- Diffusion based gelation of alginate: the diffusion of Ca^{2+} from an external source into the NaAlg solution causes the gelation of alginate polymer chain from the interface onwards. This is marked by fast gelling kinetics, which is common in the extrusion of alginate beads for use of cell encapsulation, and generally produces inhomogeneous gels.

- Internal gelation: an insoluble form of a calcium salt, such as Ca-EDTA or $CaCO_3$ is dispersed within a solution of NaAlg. The slow gelation of alginate is then initiated by the addition of δ-gluconolactone, which hydrolyses in water and releases H^+ ions. This then reacts with insoluble calcium salt and slowly releases the calcium ions into the solution to initiate homogeneous cross-linking of alginate (**Figure 2.10**).

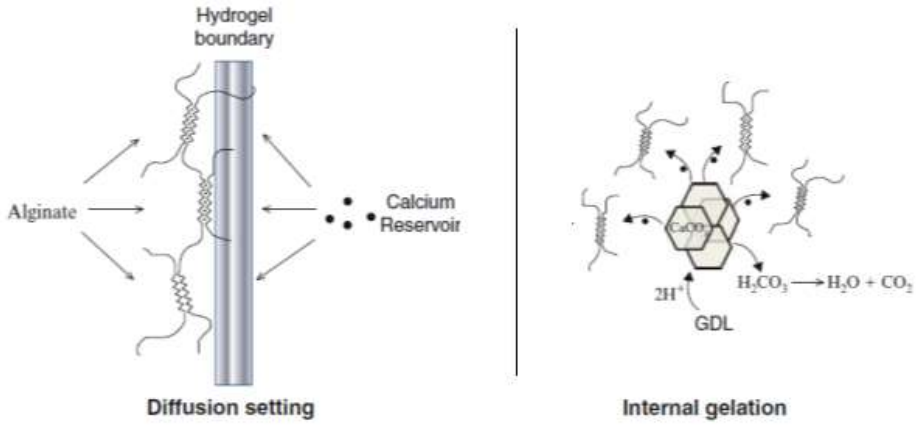

Figure 2.10: Diffusion and internal gelation setting methods for alginate [31]

To encapsulation MOI within alginate, the MOI can be dissolved within the NaAlg solution prior to gelation. This would result in formation of alginate gel beads with the MOI encapsulated within the gel network [59].

2.4 Limitations of current fabrication methods

The common issue relating to methods of fabricating PLGA microparticles, includes the leaching of water soluble drugs from the W_{int} phase to W_{ext} phase, resulting in low encapsulation efficiency [3]. Also, given the nature of the organic solvents used to dissolve the polymer in the oil phase, and also the hydrophobic polymers used (PLGA and PLLA), this often causes protein stability issues due to the solvent–water interfaces, during fabrication, storage and incubation [7, 60].

Alternate composite gel–PLGA particulate fabrication methods were reported in literature for further mitigation on encapsulation efficiency issues [11-13]. Such particulate DDS systems either have hydrogel material dispersed within matrix of the fabricated microparticle, [12] or on the microparticle surface [11]. It is noted that in these methods, the hydrogel material have to be pre-fabricated in an extra step, requiring further effort and time for microparticle fabrication.

Chapter 3 Materials and Methods

3.1 Materials

Poly (DL-lactide/glycolide) ratio 50:50 (Intrinsic viscosity IV 1.03), Poly (L-Lactide) (PLLA; IV 2.4) were purchased from Purac Biomaterials; Alginic acid sodium salt, from brown algae; Span® 80, Poly(vinyl alcohol) (PVA) (molecular weight 30-70 kDa); trisodium citrate; trifluoroacetic acid; calcium chloride; metoclopramide HCl (MCA); Bovine Serum Albumin; Lysozyme from chicken egg white were acquired from Sigma-Aldrich. Dichloromethane (DCM) and acetonitrile were obtained from Tedia Co Ltd. Sodium chloride was obtained from J.T.Baker Ltd. Phosphate Buffer Saline (PBS) (pH 7.4) was obtained from OHME Scientific Pte Ltd Singapore. All items were used as received. Bicinchoninic acid assay kit was obtained from Pierce, Thermos Scientific.

3.2 Fabrication

3.2.1 Fabrication of microparticles

3.2.1.1 Non drug-loaded particles

A modified double emulsion solvent evaporation technique was developed, to fabricate non-drug-loaded Alg-PLGA MP.

Before emulsification and solvent evaporation, the below two polymer solutions were prepared:

- PLGA/DCM solution: 10% (w/v) PLGA was dissolved within DCM, and Span80 (1% (w/v) was also added to stabilize the primary w/O emulsion.

- Sodium alginate (NaAlg) solution of 4.5% (w/v) was prepared by dissolving NaAlg in water. Sodium chloride (NaCl, 1.35 M) was also added to function as an osmolyte for the case of non-drug loaded microparticle fabrication.

A schematic showing the overview the process is depicted in **Figure 3.1**. The NaAlg solution was initially emulsified into the PLGA solution by magnetic stirring, to first form the primary w/O emulsion. This emulsion was then further emulsified into a 100 ml aqueous solution of 0.5% (w/v) PVA, 50 mM $CaCl_2$ and 0.6 M NaCl to form a w/O/W double emulsion, with an overhead stirrer fitted with a stirrer blade. The double emulsion is then stirred mechanically for three hours at 400 revolutions per minute, to concurrently start DCM evaporation and gelation of sodium alginate. The hardened microparticles were then collected by centrifugation, washed with deionized water; freeze dried and then kept in a dry box for storage. Blank Alg-PLLA MP were fabricated in the same manner as described, with the exception that 5% PLLA was used as the polymer solution instead.

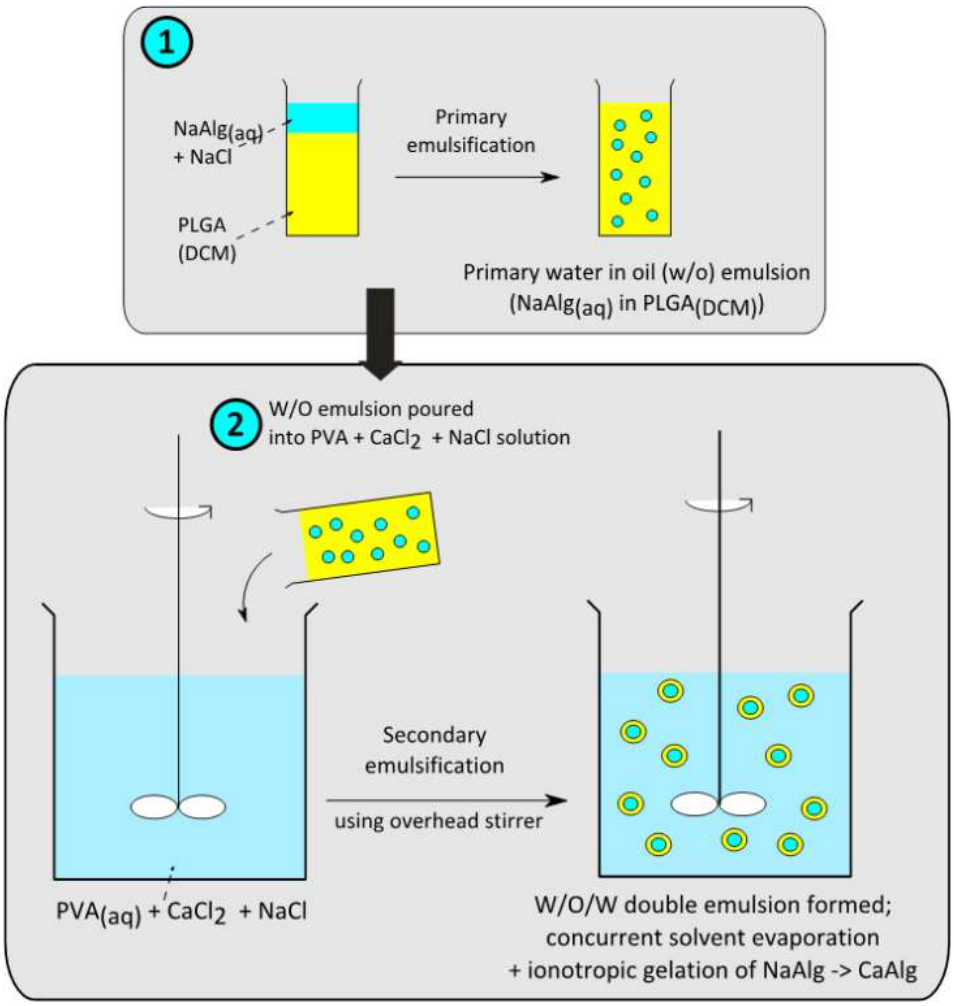

Figure 3.1: Schematic for the fabrication of Alg-Polyesteric MP.

3.2.1.2 Metoclopramide (MCA)-loaded microparticles

For MCA-loaded microparticles, MCA was first dissolved in the NaAlg solution for a 20% (w/w) theoretical drug loading. NaCl was excluded from the internal and external aqueous phase during solution preparation. Microparticles were then fabricated in the same method described for blank Alg-PLGA MP and Alg-PLLA MP. Neat MCA-loaded PLGA and PLLA microparticles were also fabricated for comparison with MCA-loaded Alg-Polyesteric MP. In this case, NaAlg was not dissolved in the internal aqueous phase prior to emulsification.

The variation of parameters for the different Alg-Polyesteric MP fabricated is shown below in **Table 3.1**.

Ref	W_{int} phase		Oil phase	W_{ext} phase			Remarks
	Encapsulant	[NaCl] (M)	Polymer	[NaCl] (M)	[$CaCl_2$] (mM)	Volume (ml)	
1A	**-**	1.35	10% PLGA 50:50 IV 1.0	0.6	50	100	Non-drug loaded Alg-Polyesteric MP
1B	**-**	1.35	5% PLLA IV 2.4	0.6	50	100	
1C	**MCA**	-	10% PLGA 50:50 IV 1.0	-	50	100	MCA-loaded Alg-Polyesteric MP
1D	**MCA**	-	5% PLLA IV 2.4	-	50	100	
1E	**-**	1.35	10% PLGA 50:50 IV 1.0	0.6	50	100	Sonicator probe used for primary emulsification
1F	**MCA**	-	10% PLGA 50:50 IV 1.0	-	50	50	Variation of W_{ext} volume
1G	**MCA**	-	10% PLGA 50:50 IV 1.0	-	50	150	
1H	**MCA**	-	10% PLGA 50:50 IV 1.0	-	50	200	
1I	**MCA**	-	10% PLGA 50:50 IV 1.0	-	50	250	

Table 3.1: List of batches fabricated for non-drug loaded and MCA-loaded Alg-Polyesteric MP

3.2.1.3 Protein-loaded microparticles

For fabrication of lysozyme (LYZ)-loaded microparticles, LYZ was first dissolved in water and then subsequently used to dissolve NaAlg, in order to produce an aqueous solution for a theoretical lysozyme loading of 10% (w/w). Microparticles were then fabricated in the same protocol described for MCA-loaded Alg-PLGA MP and Alg-PLLA MP. For BSA-loaded microparticles, LYZ was substituted with BSA. Variation in parameters for protein-loaded microparticle fabrication were also made and referenced in **Table 3.2.** Neat protein-loaded PLGA and PLLA microparticles were also fabricated for comparison with protein-loaded Alg-Polyesteric MP. In this case, NaAlg was not dissolved in the internal aqueous phase prior to emulsification.

Ref	W_{int} phase	Oil phase	W_{ext} phase		Remarks
	Encapsulant	Polymer	[$CaCl_2$] (mM)	Volume (ml)	
2A	Lysozyme	10% PLGA 50:50 IV 1.0	50	100	Lysozyme-loaded Alg-Polyesteric MP
2B	Lysozyme	5% PLLA IV 2.4	50	100	
2C	BSA	10% PLGA 50:50 IV 1.0	50	100	BSA-loaded Alg-Polyesteric MP
2D	BSA	5% PLLA IV 2.4	50	100	
2E	BSA	10% PLGA 50:50 IV 1.0	10	100	Variation of [$CaCl_2$]
2F	BSA	10% PLGA 50:50 IV 1.0	25	100	
2G	BSA	10% PLGA 50:50 IV 1.0	75	100	
2H	BSA	10% PLGA 50:50 IV 1.0	100	100	
2I	BSA	10% PLGA 50:50 IV 1.0	50	75	Variation of W_{ext} volume
2J	BSA	10% PLGA 50:50 IV 1.0	50	150	
2K	BSA	10% PLGA 50:50 IV 1.0	50	250	

Table 3.2: List of batches fabricated for LYZ- loaded and BSA-loaded Alg-Polyesteric MP

3.2.2 Fabrication of Calcium Alginate (CaAlg) beads

MCA-loaded calcium alginate (CaAlg) beads were made to compare the drug release behavior with Alg-Polyesteric MP. The beads were extruded with a syringe needle, with a 4.5% (w/v) NaAlg solution dissolved with MCA for 20% theoretical loading, into a 50 mM $CaCl_2$ cross-linking bath. Beads were then gelled in the bath for a time of 3 hours, before being used for drug release studies. LYZ-loaded and BSA-loaded CaAlg beads of 10% theoretical loading are similarly produced.

Blank CaAlg beads were similarly made, with different immersion times in a $CaCl_2$ bath for purpose of FT-IR spectroscopy to examine the changes in IR absorption with increased exposure to Ca^{2+} ions. Exposure time to Ca^{2+} ions was varied between 3, 15, 30, 60 and 180 minutes.

3.3 Characterization

3.3.1 Material characterization

3.3.1.1 Scanning Electron Microscopy (SEM)

Microparticles fabricated, were imaged with a JEOL 6360A scanning electron microscope with a JED2300 X-Ray Energy Dispersive Spectroscopy (EDX) attachment. For cross-section morphology of microparticles fabricated, microparticles were placed on double sided carbon tape, dipped into liquid nitrogen for a short while, before a surgical blade is used to make cuts across the mounted microparticles. To visually distinguish between the CaAlg hydrogel-core and the polyesteric-shell, cross-sectioned particles after imaging,

were left in trisodium citrate (0.1 M) overnight to dissolve the CaAlg hydrogel. It is noted that citrate ions sequestering the calcium ions, causes dissolution of CaAlg hydrogel [34]. The microparticles were then rinsed and air-dried before imaging again with the SEM.

3.3.1.2 FT-IR characterization

A Nicolet Continuμm (Thermo Electron) microscope connected to a FT-IR spectrometer, was used to visually identify the components of the Alg-PLGA MP, through infra-red spectroscopy. The core and shell of the Alg-PLGA MP after cross-sectioning were separated with tweezers and placed on a reflective substrate (glass slide coated with gold). FT-IR spectra were collected from 4000 cm^{-1} to 650 cm^{-1} in reflectance mode. Spectra of the CaAlg beads and PLGA were also collected for comparison.

FT-IR spectroscopy was also used to characterize CaAlg gel cores from Alg-PLGA MP fabricated with different volumes of external water phase and also CaAlg beads gelated with different Ca^{2+} exposure time. The alginate gel cores from Alg-PLGA MP were first obtained by dissolving off the shell, through immersion of microparticles in DCM under ultra-sonication, and then subsequently vacuum dried. The Perkin Elmer Spectrum FT-IR spectrometer is then used to characterize the gel cores and gel beads obtained by embedding the material within KBr pellets, running infra-red scans in transmission mode. Spectra were obtained from 4000 cm^{-1} to 400 cm^{-1} with an interval of 0.5 cm^{-1}.

3.3.1.3 Raman spectroscopic mapping with BTEM algorithm

Spectroscopy mapping with Raman signals from samples and the use of the BTEM algorithm was used to map the spatial location of polymers and the drugs loaded within the microparticles fabricated. An In-Via Reflex, Renishaw Raman microscope equipped with a near infrared enhanced deep depleted thermoelectrically Peltier-cooled CCD detector array (576x38g pixels) and a Leica microscope was used for the collection of Raman spectra. The cross-sectioned microparticles were irradiated with a 785 nm near infra-red diode laser of approximately 20 mW under a 20x microscopic objective, and measurements were collected in step size interval of 5 um within a grid area of 400 x 200 um. The signals were collected via an 1800 groove/mm static dispersive grating from 300-1900 cm^{-1}, with each acquisition time for about 35s per spectra.

Pre-processing of the spectra, including the removal of spikes from cosmic rays, was performed before the collected spectra are analyzed with the band target entropy minimization (BTEM) algorithm. The BTEM algorithm was used to reconstruct pure component spectral estimates [61, 62]. Each normalized pure component spectra of the underlying constituents were reconstructed and relative contributions of each measured point of the signals was calculated by projecting them back onto the baseline corrected and normalized data set. A color-coded scale represents the intensity of each component recovered in a score image, where summation of intensities (color-coded scale) of all components at each grid pixel is equated to unity. The score images were then used to depict the distribution and the semi-quantitative content for all observed component in the microparticles [63].

3.3.2 Encapsulation quantification techniques

3.3.2.1 Drug loading

Actual drug loading and encapsulation efficiency of the microparticles fabricated are defined as below:

Actual Drug Loading %(w/w)
= 100% x (Mass of drug loaded / Total polymer mass)

Encapsulation Efficiency (%)
= 100% x (Actual Drug Loading / Theoretical Drug Loading)

Actual drug loading of MCA loaded microparticles was determined, by digesting 5 mg of microparticles in 1 M NaOH in a sonication bath, for 10 min in an 80 ºC water bath. The solution was then neutralized and filtered before analysis. A reverse phase high performance liquid chromatography (HPLC) method, using the Agilent 1100 HPLC system with a XDB-C18 column was used to determine the drug concentration in the solution. 0.1% (v/v) trifluoroacetic acid and acetonitrile was used as the mobile phase, and the feed through of the mobile phases through the column was done in gradient mode and detected with a visible wavelength detector at 309 nm.

For protein-loaded microparticles, an alternative protein extraction method was used. 10 mg of microparticles were weighed in triplicate and then added to acetonitrile, vortexed and placed in an ultrasound bath to remove the polymer shell of the microparticles. The resultant suspension is then centrifuged and the supernatant removed. Acetonitrile is then added again and the process was repeated for another 2 times before the residue was then

dried in a vacuum oven. The dried residue is solubilized in PBS and the resultant solution was assayed using a bicinchoninic acid (BCA) assay.

3.3.2.2 Drug release studies

MCA-loaded microparticles (5 mg) were added to 5 ml phosphate buffer saline (PBS) in vials, placed in a 37 ºC orbital shaking incubator. At pre-determined time intervals, 1 ml of the release medium was extracted from the vial and analyzed for concentration of MCA released. The vials were then replenished with same volume of fresh PBS after drawing the sample aliquot. An UV-Visible Spectrophotometer (Shimadzu UV-2501) was used to measure the MCA concentration through by measuring the absorbance at detection wavelength 309 nm.

For protein-loaded microparticles, 10 mg of particles are similarly weighed and immersed in vials of Dulbecco PBS for release. The release medium is similarly extracted for characterization at set time intervals. The protein concentration of the release aliquot was determined using the BCA assay kit.

3.3.3 Protein bioactivity studies

3.3.3.1 Micrococcus lysodeikticus assay for lysozyme lysing activity

The bioactivity of lysozyme in the control and release aliquots of LYZ-loaded Alg-Polyesteric MP was characterized through its lysing activity of Micrococcus lysodeikticus (ML) cells. 0.5 mg/ml suspension of deactivated lyophilized ML cells was suspended in 66 mM pH 7.0 potassium phosphate buffer at 25 °C. 200 µl of ML suspension were then added into the wells of a 96 well plate, each containing 50 µl of 10 ug/ml of either the control samples of lysozyme or the release aliquots. The turbidity of the suspension is then tracked, by measuring the absorbance at 450 nm with a Tecan M-100 well plate reader at every minute for a period of 5 minutes. The measured absorbance values were then plotted against time and compared with those for native lysozyme.

3.3.3.2 SDS-PAGE

Sodium Dodecyl Sulfate Polyacrylamide gel electrophoresis (SDS-PAGE) was conducted on released aliquots to examine for fragmentation of BSA post release. Samples were reduced with DTT at 70 ºC for 10 minutes, before loading into sample wells of NuPAGE BisTris 4-12% precast gradient gels. A potential difference was applied to the gel for electrophoresis at 120 V, 1.5 hours with 30 W of power applied. Gels were then stained with a SimplyBlue Commasie Blue stain for an hour and then further de-stained to resolve the bands against a clear background.

3.3.3.3 Circular Dichronism

The secondary structure of BSA native control and release aliquots from BSA loaded particles were analyzed by collecting circular dichronism (CD) spectra using a Jasco J-815 spectropolarimeter. Scans were made in the far-UV region from 190-260 nm, using a quartz cuvette of 1 mm path-length, with an accumulation of 3 scans per aliquot. Scan parameters used included a 0.2 nm data pitch, a data integration interval of 4 sec, bandwidth of 1.0 nm and a scan rate of 50 nm/min.

Chapter 4 Results and Discussion

4.1 Blank and MCA-loaded Alg-PLGA and Alg-PLLA MP

In this section, the morphology of the blank and MCA-loaded core-shell microparticles fabricated will be discussed. The drug loading and release behavior was also compared with MCA-loaded CaAlg beads.

In addition, various fabrication conditions affecting the formation of the core shell microparticles will also be discussed, including the primary emulsification power used and the volume of W_{ext} used.

4.1.1 Particulate cross-section morphology

The formation of microparticles was examined by scanning electron microscopy (SEM) and the various components were verified via FT-IR spectroscopy, selective dissolution of the particulate components and Raman mapping.

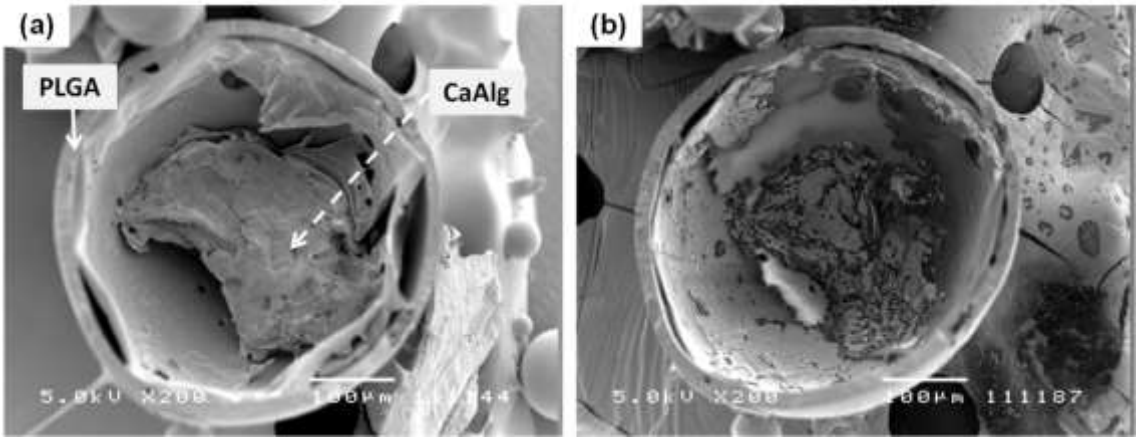

Figure 4.1.1: Electron microscopy images of Alg-PLGA MP, depicting the same microparticle before (a) and after addition of citrate (b) [63]

Alg-PLGA MP fabricated was shown to consist of an alginate core and a PLGA shell structure. The cross-section view of Alg-PLGA MP is shown in **Figure 4.1.1a**, depicting a core-shell structure within the microparticle. When this cross-sectioned microparticle was immersed in trisodium citrate, and viewed again under the SEM, the core portion was shown to have been removed (**Figure 4.1.1b**). As the citrate ion can chelate and sequester Ca^{2+} ions from CaAlg, this causes the gel structure of CaAlg to be dissolved [34], whereas the PLGA component remained intact and unaffected by the action of the citrate ion. This indicates that the core portion of the microparticle that was removed via citrate treatment was calcium alginate (CaAlg).

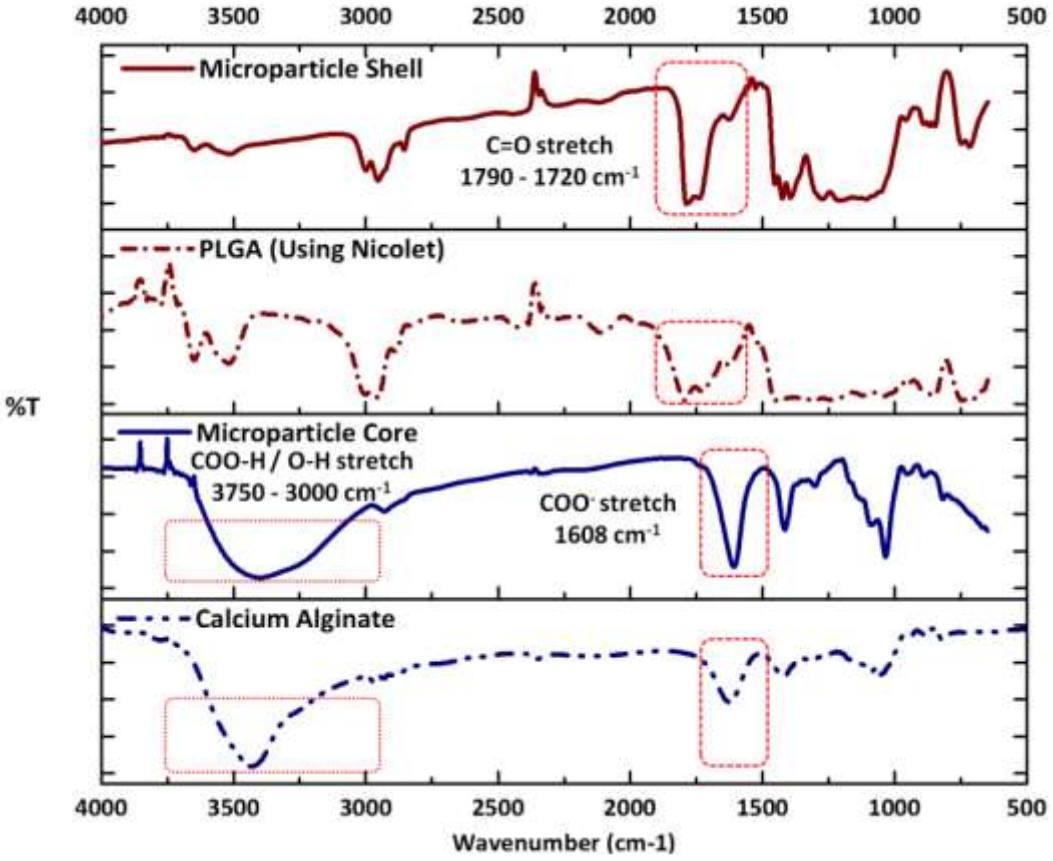

Figure 4.1.2: Infra-red spectra of the different components of Alg-PLGA MP [63]

The infra-red (IR) spectra of the microparticle component, with the spectra of PLGA and a CaAlg bead are shown above in **Figure 4.1.2**. It is seen here that IR spectra of the microparticle core and shell matched with the reference spectra of CaAlg and PLGA respectively. The strong broad peak at around 3500-3000 cm^{-1} arising from the gel core, distinguishes it from the material in the microparticle shell. This is representative of the O-H stretch of repeated -COOH and –OH units on the alginate polymer chain. Also, the carboxylate COO^- stretching absorption peak is also seen around 1608 cm^{-1} for the CaAlg core [63-65]. The doublet seen between 1790-1720 cm^{-1} for the shell, on the other hand, is representative of the C=O carbonyl stretch of the lactide and glycolide groups arising from PLGA.

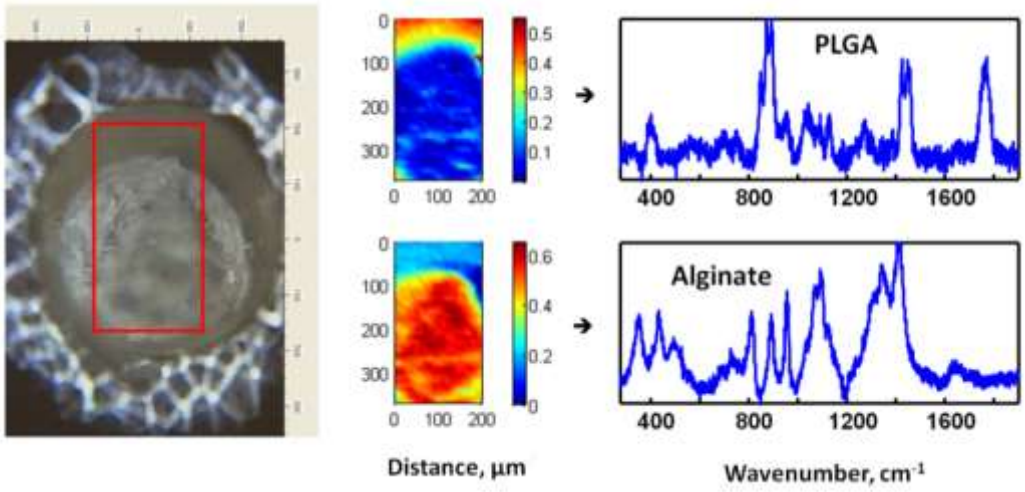

Figure 4.1.3: Optical microscopy image of a cross-sectioned Alg-PLGA MP, with the Raman mapping results corresponding to the cross-section of the microparticle [63]

The Raman mapping of a cross-sectioned microparticle and its associated pure component BTEM spectra estimates are shown in **Figure 4.1.3**, indicating the location of each microparticle component. The core of the cross-sectioned microparticle is shown to be CaAlg, distinct from the surrounding PLGA shell. Basing on SEM imaging, IR spectra

and Raman mapping, it is hence conclusive that the microparticles formed had core-shell geometry of CaAlg and PLGA, respectively.

Alg-PLLA MP fabricated is also shown to be formed with a similar core-shell structure depicted by Alg-PLGA MP. As shown, **Figure 4.1.4a** shows the cross-section image of Alg-PLLA MP with a visual core and shell differentiation. The same cross-sectioned particle with the gel core after citrate dissolution was also shown to be removed (**Figure 4.1.4b**), indicating that the core was removed after citrate dissolution.

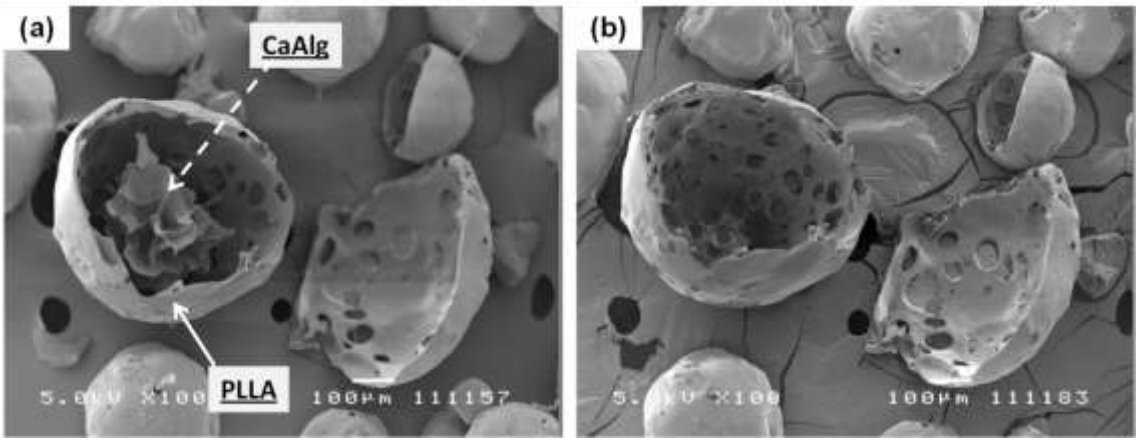

Figure 4.1.4: Electron microscopy images of Alg-PLLA MP, depicting the same microparticle before (a) and after addition of citrate (b) [63]

The Raman mapping of Alg-PLLA MP (**Figure 4.1.5**), likewise shows the localization of the different polymeric components, confirming the core and shell to be alginate and PLLA respectively. It is noted as well that carbon was also detected, as the particles were mounted on carbon tape during Raman mapping.

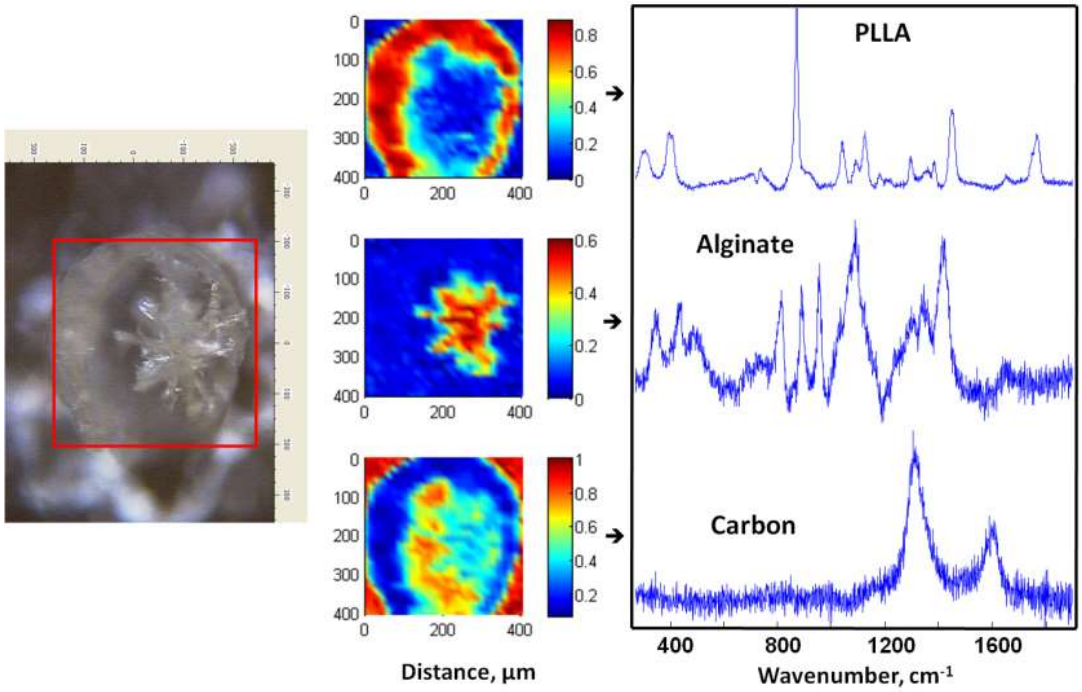

Figure 4.1.5: Optical microscopy image of a cross-sectioned Alg-PLLA MP, with the Raman mapping results corresponding to the cross-section of the microparticle [63]

For the loading of MCA within the core-shell microparticles discussed above, MCA was dissolved within the NaAlg solution before emulsification. The images below shows the cross-section of a MCA-loaded Alg-PLGA MP (**Figure 4.1.6**):

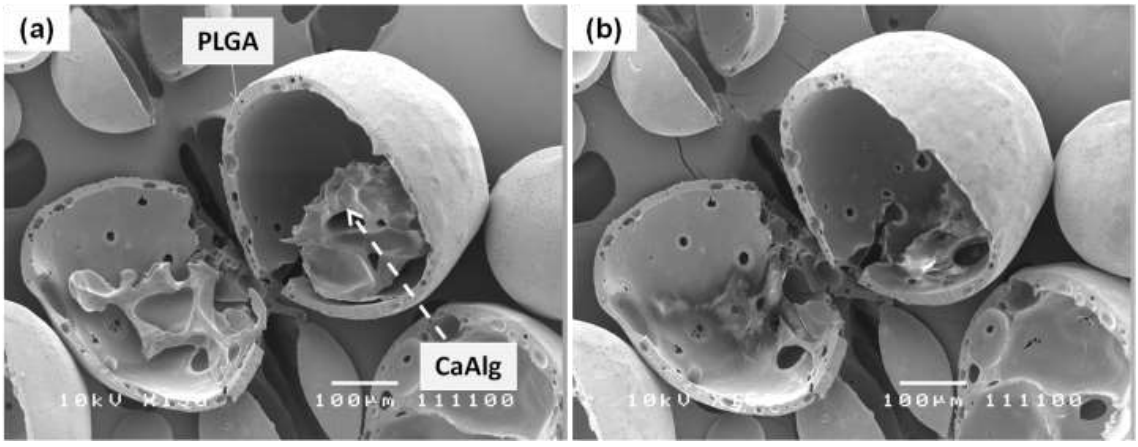

Figure 4.1.6: Electron microscopy images of MCA-loaded Alg-PLGA MP, depicting the same microparticle before (a) and after addition of citrate (b) [63]

As observed in blank Alg-PLGA MP and Alg-PLLA MP formed, a similar core-shell structure was formed. In addition, Raman mapping indicates a strong MCA signal from the particle core, and PLGA in the shell (**Figure 4.1.7**). Citrate dissolution of the core of the microparticles further indicates that the core is CaAlg (**Figure 4.1.6b**). It is noted though, that the Raman spectrum of CaAlg was not recovered. This was partly due to fluorescence interference and Raman scattering from MCA, subsequently resulting in a relatively stronger signal, which could have overshadowed any CaAlg present [63].

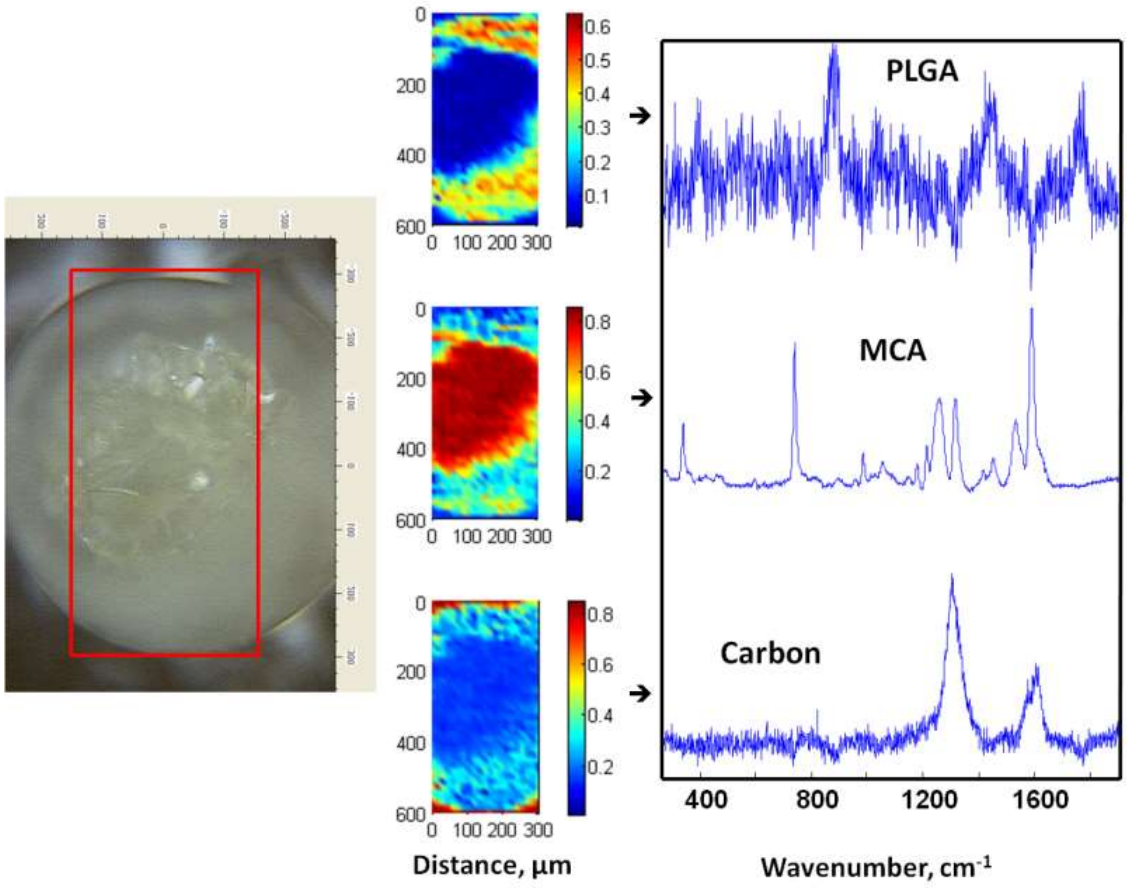

Figure 4.1.7: Optical microscopy image of a cross-sectioned MCA-loaded Alg-PLGA MP, with the Raman mapping results corresponding to the cross-section of the microparticle [63]

In the case of MCA-loaded Alg-PLLA MP, a similar core-shell structure was also replicated, when PLGA was used to form the shell of the microparticle (**Figure 4.1.8**).

Likewise, the gel dissolution occurred as well when the same particle was subjected to the citrate dissolution test.

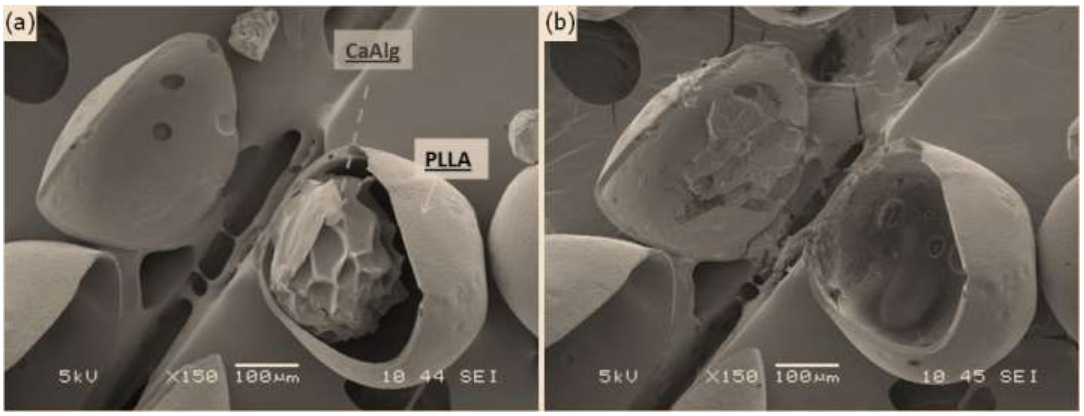

Figure 4.1.8: Electron microscopy images of MCA-loaded Alg-PLLA MP, depicting the same microparticle before (a) and after addition of citrate (b) [63]

Hence, it is shown that microparticles fabricated using this technique have a core-shell structure, where the embedded alginate gel core was located within a hydrophobic shell polymer of either PLGA or PLLA. Drugs to be encapsulated within this particulate architecture, can be loaded by dissolving them in the internal aqueous NaAlg phase before emulsification, and subsequently localizing them within the CaAlg gel core of the particles formed. This single step process also eliminates the need for prefabrication of gel material prior to emulsification as seen in prior work.

It is also noted that the gelation of CaAlg within the microparticles occurred during the fabrication process. It appears that the concurrent processes of solvent extraction of the PLGA/DCM phase, and the ionotropic gelation of alginate in the internal water phase occured during the secondary emulsification of the double emulsion. This is evident with the in-situ formation of a gel core material within an enveloping shell polymer material, hardened via the removal of DCM. Since alginate can be gelled in the presence of

calcium ions [31, 33], the calcium ions would have diffused from the external water phase into the internal phase to effect the formation of a CaAlg gel core [63].

It is also noted that varying the polymer shell material can be achieved by dissolving a different polymer in the solvent used for the oil phase. In the above examples shown, we have shown that fabrication of Alg-PLLA MP was achieved by simply dissolving PLLA instead of PLGA to form a PLLA/DCM polymer solution. This indicates that microparticles with a different polymer shell can be changed, by just simply dissolving a target polymer of interest in the organic solvent.

4.1.2 Drug loading and release of MCA-loaded Alg-Polyesteric MP

The encapsulation efficiency of MCA in PLGA and PLLA microparticles fabricated with and without the inclusion of CaAlg is compared in **Table 4.1.1**. An almost double in increase in encapsulation efficiency of MCA was observed for the core-shell microparticles, when compared to the neat monolithic polyesteric microparticles.

MCA Encapsulation Efficiency (%)		
Shell Polymer / Microparticle Type	**Monolithic matrix**	**Alginate core + Polymeric shell**
PLGA	30.1 ± 2.40	59.96 ± 13.82
PLLA	32.26 ± 1.99	66.54 ± 2.23

Table 4.1.1: Encapsulation Efficiencies of MCA loaded microparticles of different polymer types, neat and Alg-Polyesteric MP [63]

Since encapsulation efficiency is correlated to the drug leach to the W_{ext} phase in emulsion solvent evaporation fabrication methods [30], the presence of a hydrophilic

polymer like alginate can better retain and associate with hydrophilic drugs, as compared to the more hydrophobic PLGA. This hence resulted in improved drug loading efficiency for the fabricated Alg-Polyesteric MP.

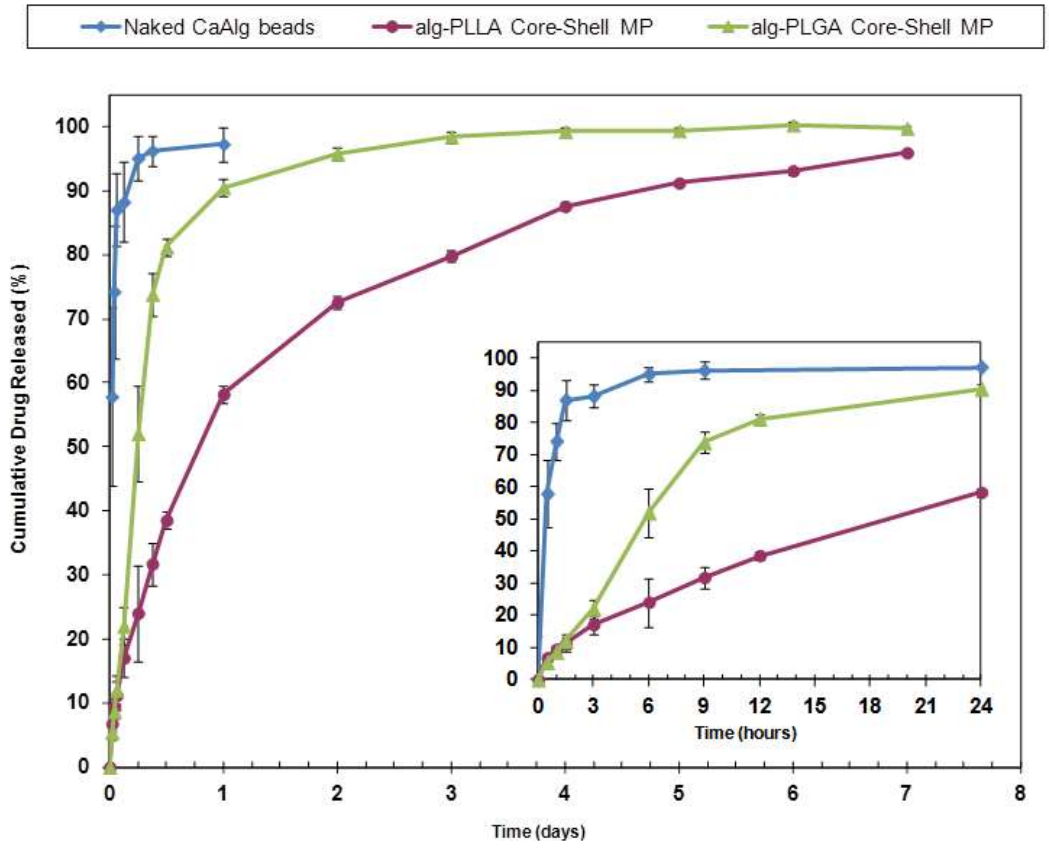

Figure 4.1.9 : Release profile of MCA from MCA-loaded Alg-Polyesteric MP and CaAlg beads across 7 days (main plot), and a close up of the initial 24 hours (inset) [63]

The release profile for the MCA-loaded Alg-PLGA MP, Alg-PLLA MP and naked CaAlg beads are shown in **Figure 4.1.9**. MCA-loaded naked CaAlg beads showed a complete drug release within 6 hours, while Alg-Polyesteric MP exhibited a suppressed initial burst in the first 1 day. This was followed by sustained release till to 4 and 7 days, respectively for PLGA and PLLA shell Alg-Polyesteric MP.

It was noted that Alg-PLLA MP exhibited a more sustained release as compared to Alg-PLGA MP. It was then also observed that when fitting the release data with the power law (**Table 4.1.2**), a lower n exponent value for Alg-PLLA MP was observed, when compared to Alg-PLGA MP.

Particle type	Release Exponent n	Linear Correlation Coefficient R^2
Alg-PLGA MP	0.8194	0.9686
Alg-PLLA MP	0.5104	0.9911

Note: Power law is defined as $M_t/M_\infty = k(t)^n$,
where M_t/M_∞ is the fraction of total drug release at time t, k = constant, n = release exponent

Table 4.1.2: Fitting results of release with the power law [63]

This difference in the release exponent, could be due to the semi-crystallinity of PLLA, which causes the retardation of the MCA release rate, when compared to amorphous PLGA, which has a more open polymer network [66]. Hence, it is expected that release kinetics of Alg-Polyesteric MP can be tuned by choosing a suitable polymer as the polymer shell.

4.1.3 Other fabrication conditions affecting particulate formation

In this section, other miscellaneous conditions affecting the microparticle formation are examined. This serves to examine how certain conditions when changed, affects the primary emulsification method and particle hardening process.

4.1.3.1 Primary emulsification factor

The primary emulsification method was changed to examine the effect on particulate cross-section morphology. In this case, a sonication probe was used to form the primary w/O emulsion, instead of magnetic stirring. It was observed that the particles formed have much smaller internal cavities with some of them filled by small bits of CaAlg. Unlike particles fabricated with magnetic stirring, a larger cavity with a central gel core was not formed (**Figure 4.1.10**).

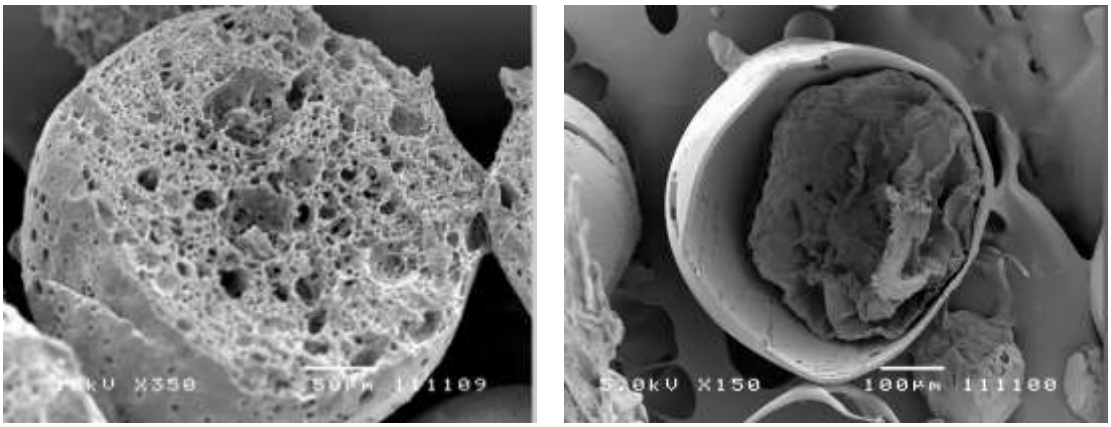

Figure 4.1.10: Cross-section of microparticles formed primary emulsification with a sonication probe (left) and magnetic stirring (right)

It is noted that a sonication probe emulsifies by the cavitation effect and produced a finer w/O emulsion with smaller W_{int} droplets, as opposed to a magnetic stir bar which emulsifies by rotational shearing action. Hence, it can be seen here that the W_{int} droplets did not coalesce before particulate hardening took place, resulting in formation of a

microparticle with a porous cross-section. This is in contrast to microparticles fabricated with magnetic stirring, where a central hydrogel core was formed instead.

Since the cross-section of a microparticle formed by a double emulsion ESE method is representative of the state of the w/O droplets and the location of W_{int} droplets prior to hardening, this indicates that the hardening rate is in competition with the speed the W_{int} droplets coalesce, which would then affect the particulate cross-section morphology.

4.1.3.2 Volume of external water phase

To examine the effect of change in volume of the W_{ext} phase, different volumes of W_{ext} phase was used for solvent evaporation during particulate fabrication. The CaAlg gel core was recovered from the fabricated Alg-PLGA MP microparticles via DCM dissolution of the shell, and the gel bits were then characterized using FT-IR spectroscopy.

The collected FT-IR spectra are shown in (**Figure 4.1.11a**). It is observed that with a lower volume of W_{ext} phase used, the change in –OH stretch at 3500 cm^{-1}, where the tip of the peak with respect to the –OH shoulder is, becomes increasingly pronounced.

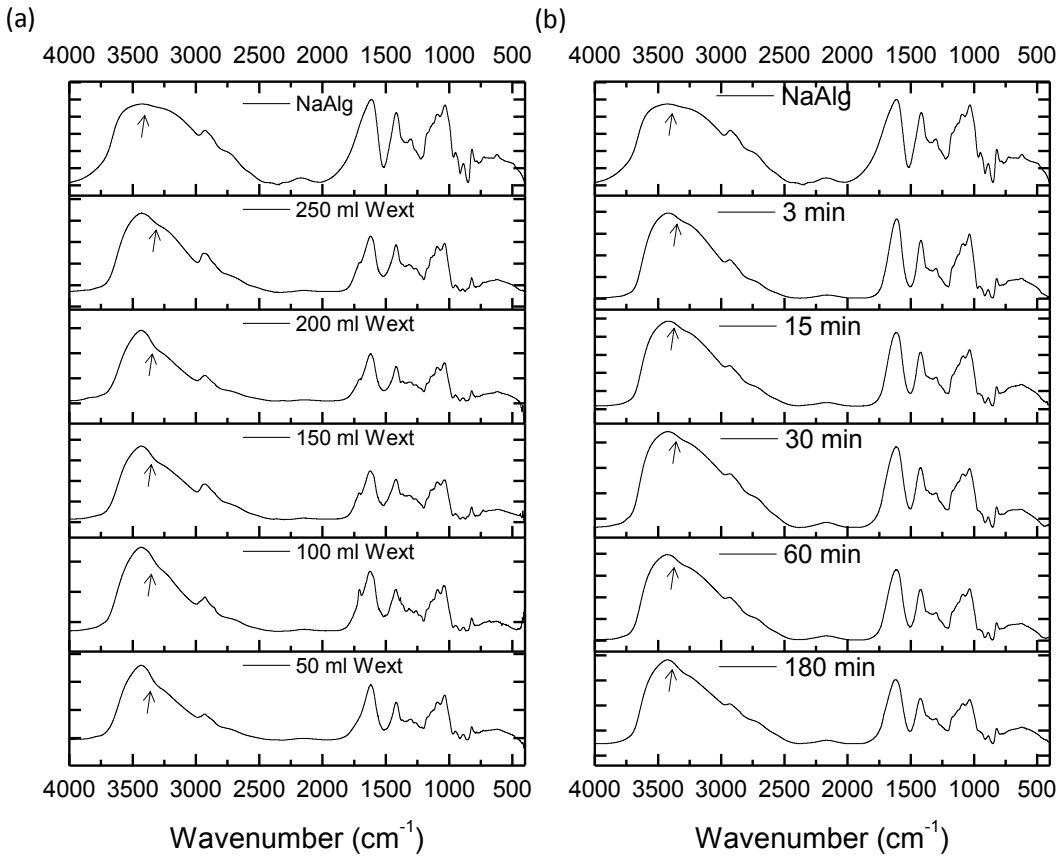

Figure 4.1.11: FT-IR spectra of (a) CaAlg gel core recovered from particles with different volume of W_{ext} phase used for particle fabrication, and (b) CaAlg beads gelated with different Ca^{2+} gelation times.

This change is similarly observed in CaAlg beads, when bead immersion time in $CaCl_2$ increases (**Figure 4.1.11b**). This change in FT-IR spectra is an indication of Ca^{2+} exposure time and increased calcium cation content, as reported by Sartori et al, where an increase in Ca^{2+} exposure time resulted in a more pronounced –OH stretching peak (**Figure 4.1.12**). [64]

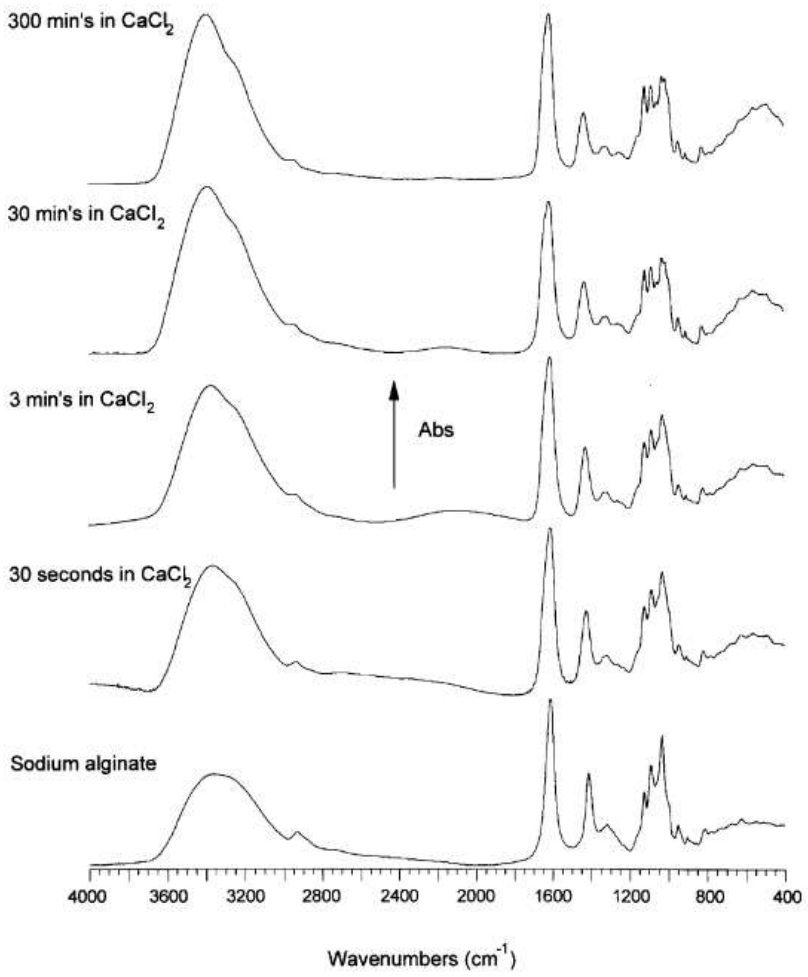

Figure 4.1.12: Comparison of $CaCl_2$ exposure time for CaAlg beads [64]

In correlation with the FT-IR spectra obtained, it appears that with decreased volume of W_{ext} phase, an increase in Ca^{2+} exposure time and content was observed. Given that the decreasing W_{ext} volume results in a slower hardening of the PLGA/DCM layer due to a slower precipitation rate, more Ca^{2+} ions in the W_{ext} water phase can then diffuse from the W_{ext} phase to the W_{int} phase during emulsification. Hence, a slower hardening rate would allow an increased time for Ca^{2+} ions to diffuse and penetrate the w/O double emulsion droplets. This difference in Ca^{2+} exposure time for NaAlg gelation, could then explain the change in FT-IR spectra observed.

4.1.4 Discussion

4.1.4.1 Characterization techniques

The various microparticles fabricated using the technique explored have a core–shell structure of a CaAlg core and a polyesteric shell. Identifying the corresponding polymer for the core and shell required using BTEM based Raman mapping to resolve the combined Raman signals from the different components of the microparticle. This helped to spatially map the different materials present, which was difficult to identify if only microscopy is used. Also, the use of citrate to sequester calcium ions in order to dissolve CaAlg, confirms further that the particle core was indeed CaAlg. This helps to conclude the presence of a core–shell structure present in the microparticle.

4.1.4.2 Particulate formation

The Alg-Polyesteric MP were fabricated using a modified double w/O/W emulsion ESE method, depicted in **Figure 3.1** and **Figure 4.1.13**. This first involves the forming the first primary w/O emulsion, by dispersing a W_{int} phase consisting of NaAlg and NaCl into an oil phase (i.e. PLGA/DCM). The w/O emulsion was then subsequently dispersed into a W_{ext} phase with PVA, $CaCl_2$ and NaCl dissolved, to form the secondary double emulsion. When secondary emulsification is initiated, this started two concurrent processes resulting in the formation of the core-shell microparticle [63].

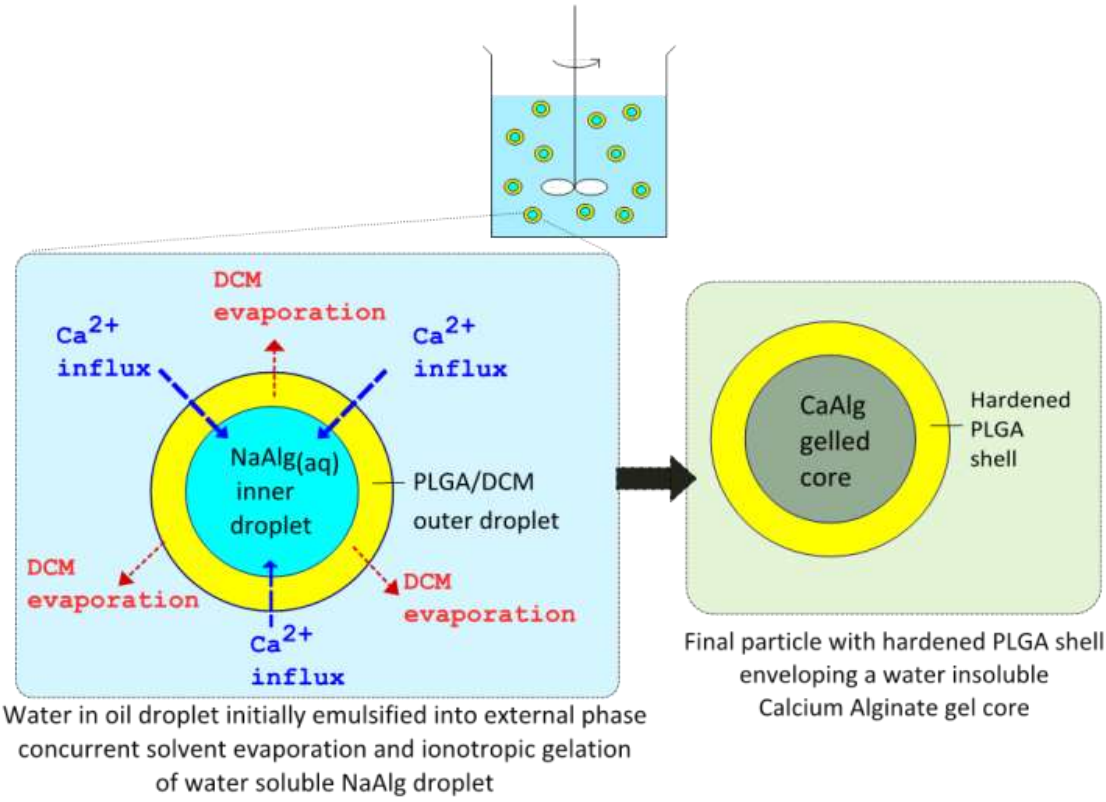

Figure 4.1.13: Principles of Alg-PLGA MP formation

One of the two concurrent processes occurring, was the removal of DCM from the w/O double emulsion droplet, resulting in the PLGA precipitation and forming the PLGA shell. This extraction initiated the hardening of the PLGA shell, by the partitioning of the solvent into the water and then evaporated from the water phase. Hence, the hardening rate and the corresponding solvent extraction rate can be controlled by varying the volume of W_{ext} phase.

The second process happening concurrently was the ionotropic gelation of the NaAlg within the W_{int} droplet. Since NaAlg can be gelated, i.e. physically cross-linked with divalent ions such as Ca^{2+} to form CaAlg hydrogel [31], Ca^{2+} influx from the W_{ext} phase into the W_{int} phase causes the alginate dissolved within the W_{int} phase to gel, forming

CaAlg. With both processes happening simultaneously, microparticles with core-shell CaAlg-PLGA geometry can be formed in a one-step fabrication step, whereby water insoluble CaAlg core is gelled in-situ within the hardening PLGA shell.

For stabilization of the w/O/W double emulsion, a hydrophobic Span80 surfactant and hydrophilic PVA surfactant stabilizes the primary w/O emulsion and disperses the secondary w/O double emulsion droplets within in the external water phase. Fabrication of particles without Span80, resulted in microparticles with inconsistent shapes and sizes. This can be attributed to the destabilizing of the double emulsion droplet in the external phase, resulting in droplet sizes of different sizes and hence different particulate sizes [63].

Given that this fabrication method relies on forming a w/O/W double emulsion, any huge osmotic pressure differences between the two water phases can cause a bulk movement of water between both phases. This affects stability of the double emulsion, which could rupture the DCM/PLGA oil layer and causing the double emulsion droplets to break [63, 67]. At the same time, the contents of the internal aqueous phase (i.e. alginate and MCA) can also leach into the external phase due to molecular migration [58]. NaCl therefore was used as an osmolyte in both W_{ext} and W_{int} phases of the w/O/W emulsion to reduce the osmotic pressure difference between the two aqueous phases of the double emulsion, while at the same time, to reduce leaching of alginate [68, 69].

It was noted that when MCA was encapsulated within the microparticles, NaCl was no longer needed during fabrication. Given alginate can form complexes with poly-cations

such as chitosan and poly-L-lysine [34, 63], it was inferred that the dissolved MCA could form a similar complex with alginate, possibly due to the presence of amine and amide groups in the drug [63]. Also, MCA dissolution may have led to an increased osmotic pressure in the W_{int} phase [70]. Hence, this would restrict contents of the W_{int} phase from leaching and increase the retention of alginate within the w/O double emulsion droplet. A drug like MCA can therefore substitute NaCl, as an osmolyte, for the fabrication of drug-loaded Alg-PLGA MP.

The gelation of NaAlg is also correlated to the permeability of Ca^{2+} ions through the PLGA/DCM layer, affected by the solvent extraction rate and the variation in W_{ext} volume. Since polymer precipitation rate is hastened with an increased volume of W_{ext} phase used, a resultant increased rate of solvent removal decreases the influx of Ca^{2+} into the W_{int} and vice versa. The difference in Ca^{2+} content with different solvent extraction rates, affirms the presence of a semi-permeable DCM/PLGA phase membrane layer, during the formation of a double emulsion [58], which impeded the penetration of Ca^{2+} ions upon hardening of the particulate shell.

It is also observed that the cross-section morphology changes, when a different primary emulsification method was used. When a finer primary w/O emulsion was formed via sonication, smaller cavities containing CaAlg were observed. This is in contrast to the larger central CaAlg core formed via magnetic stirring primary emulsification. Since the pores formed are due to voids left over by W_{int} phase droplets dispersed within the DCM/PLGA phase after lyophilization, the cavities are an indication of the W_{int} droplet

size and position prior to particle hardening. From this, it can be assumed that the particle hardening rate, in relation to the time required for the W_{int} droplets to coalesce, will affect the final cross-section morphology of the particles formed.

4.1.4.3 Drug loading and release behavior

For drug encapsulation, the MOI can be either dissolved in the W_{int} phase or the solvent/polymer oil phase before emulsification. For example, MCA was loaded by dissolving the drug in the W_{int} phase before emulsification. It was also noted that Alg-Polyesteric MP had increased encapsulation efficiency over neat polyesteric microparticles without alginate. This could be due to the encapsulation of MCA within viscous W_{int} droplets dissolved with NaAlg and gelated during fabrication, subsequently increasing retention of drugs within the W_{int} droplets and reducing out-flux of water soluble drugs during fabrication. This also indicates that the inclusion of water soluble polymer can help to improve encapsulation efficiency of drugs which are rather water soluble.

An initial study of the release behaviour compared with naked CaAlg beads was also examined. A reduced burst release was observed for Alg-Polyesteric MP when compared to naked CaAlg beads, and was due to the microparticles shell acting as a protective sheath and behaving as a membrane to control the amount of drug released. While hydrogels are known to release its contents rapidly [3, 71], the surrounding shell of PLGA or PLLA limits the water influx and becomes a rate-limiting membrane for drug diffusion.

It was also observed that each different type of polymer selected can limit the drug release rate differently, depending on the polymer's hydrophobicity, crystallinity and rate of degradation.

It is thus in hope, that the combination of a drug-loaded gel core within a polyesteric encapsulating material, will improve encapsulation efficiencies of water soluble drugs; while the polymer shell which encapsulates the drug loaded hydrogel core will limit the release of the drugs by acting as a semi-permeable membrane during release.

4.2 Protein-loaded Alg-Polyesteric MP

In this section, the loading of Alg-Polyesteric MP with lysozyme and BSA will be discussed. The cross-section of the microparticles fabricated was also examined, while encapsulation efficiency, drug release behavior and the bioactivity of the proteins loaded were examined after release.

4.2.1 Lysozyme-loaded Alg-Polyesteric MP

4.2.1.1 Cross-section morphology of microparticles fabricated

The SEM image of cross-sectioned lysozyme (LYZ)-loaded Alg-PLGA MP are shown below in **Figure 4.2.1**. The microparticles formed were observed to have CaAlg gel material dispersed within the PLGA matrix.

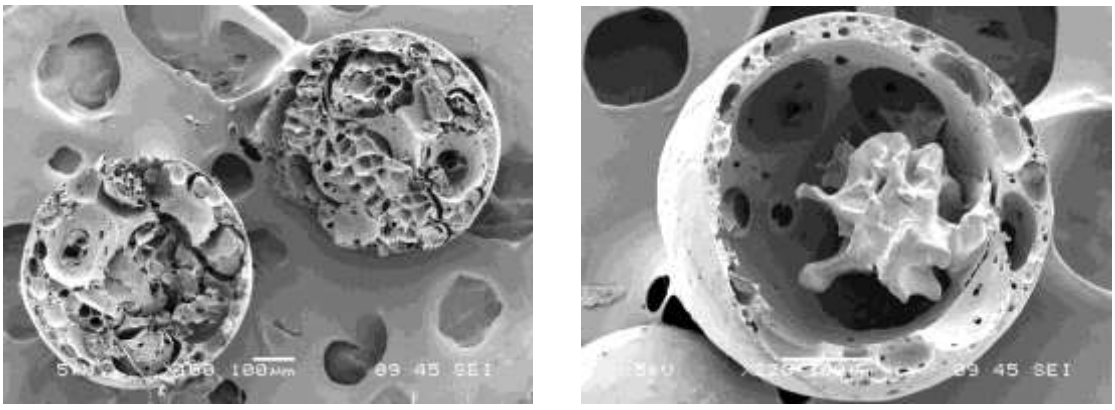

Figure 4.2.1: SEM images showing cross-section of LYZ-loaded Alg PLGA MP

The CaAlg gel portions of the microparticle were distinguished from the PLGA matrix via an EDX mapping of particles on the SEM to locate regions of calcium (**Figure 4.2.2)**. From there, it can be seen that the core of these microparticles were calcium rich, indicating the location of the CaAlg gel core material. (Carbon was detected in the

background during mapping, as microparticles were mounted on adhesive carbon tape during EDX mapping.)

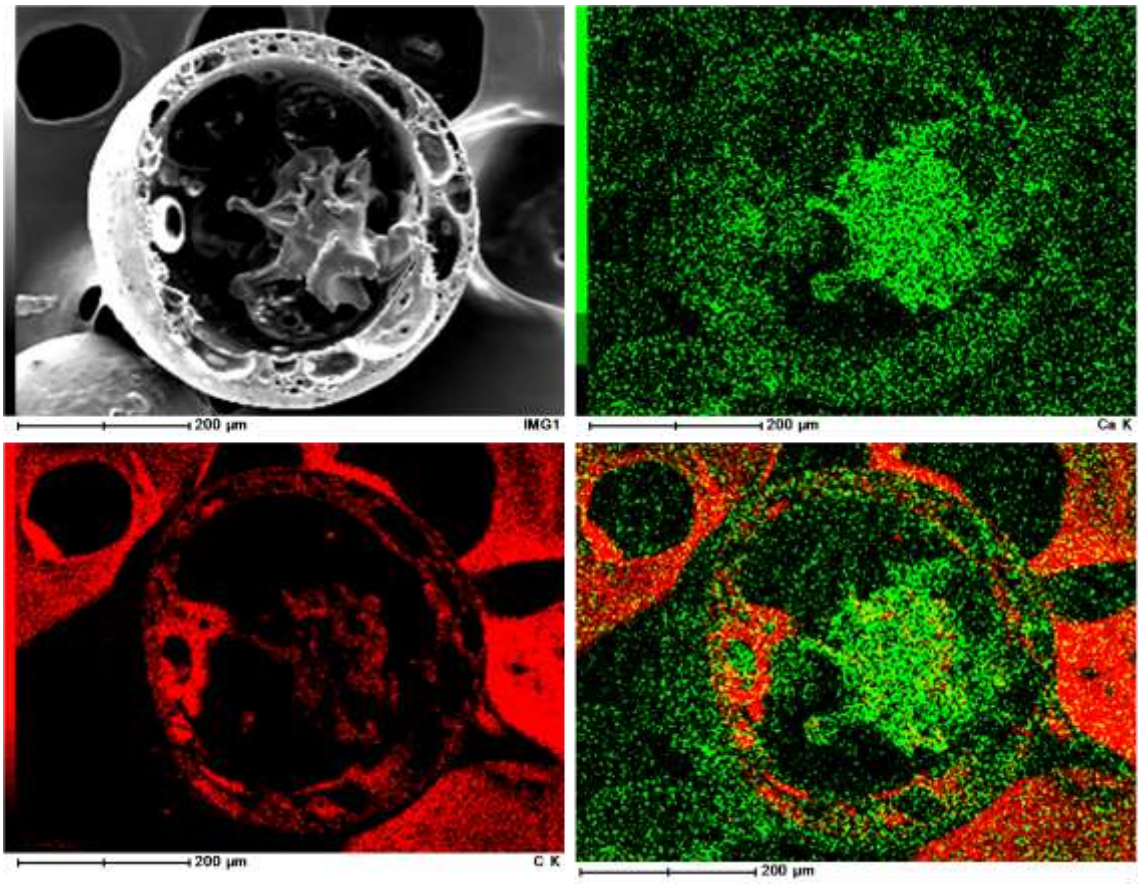

Figure 4.2.2: SEM/EDX map of a LYZ-loaded Alg-PLGA MP
(red represents location of carbon, green represents location of calcium)

LYZ-loaded Alg-PLLA MP fabricated is shown below (**Figure 4.2.3**). Likewise, the cross-sectioned microparticles have core and shell structures as seen in LYZ-loaded Alg-PLGA MP.

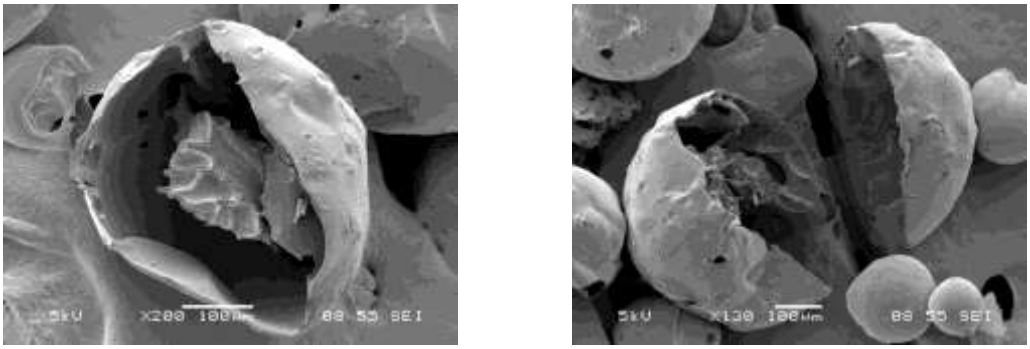

Figure 4.2.3: SEM images showing cross-section of LYZ-loaded Alg-PLLA MP

The EDX mapping of a cross-sectioned LYZ-loaded Alg-PLLA MP is shown below in **Figure 4.2.4**. Elemental calcium is shown to localize within the core of the particles, indicating the core of the microparticle consists of CaAlg, as observed for LYZ-Alg-PLGA MP.

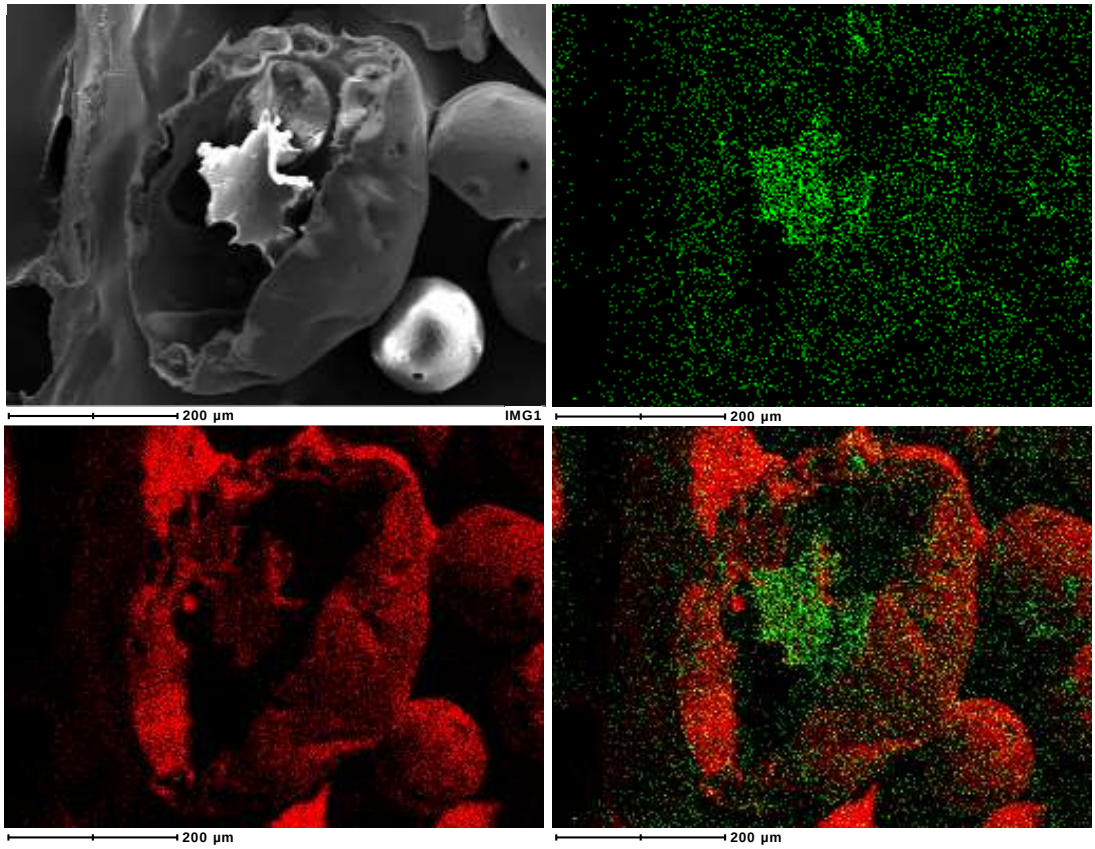

Figure 4.2.4: SEM/EDX map of a LYZ-loaded Alg-PLLA MP
(red represents location of carbon, green represents location of calcium)

4.2.1.2 Encapsulation efficiency and release from LYZ-loaded Alg-Polyesteric MP

The encapsulation efficiency of the different type of particles fabricated, are shown below in **Table 4.2**.

Lysozyme Encapsulation Efficiency (%)		
Shell Polymer / Microparticle Type	**Monolithic matrix**	**Alginate core + Polymeric shell**
PLGA	100.57 ± 8.08	83.07 ± 6.82
PLLA	84.88 ± 8.80	64.87 ± 3.74

Table 4.2.1: Loading efficiency of LYZ-Alg-Polyesteric MP, compared to neat microparticles

In terms of loading, we note that microparticles fabricated with PLGA, generally have higher encapsulation efficiency (EE) when compared to those made using PLLA. This was expected due to the slightly hydrophilic character of PLGA compared to PLLA, as a result of the presence of the GA groups, as opposed to the all LA groups found on PLLA.

It is also noted that LYZ-loaded Alg-Polyesteric MP did not have higher EE when compared to neat microparticles, as opposed to what was seen in MCA-loaded Alg-Polyesteric MP. Some of the possible reasons include leaching of the lysozyme into the W_{ext} phase, with the formation of water channels and other surface defects during fabrication as a result of osmotic pressure imbalances. Also, one can note that the amphiphilic nature of proteins may have resulted in the partitioning of lysozyme at the oil/water interfaces, which may have resulted in further leaching and contribution to a lower loading as well.

The release of lysozyme from LYZ-loaded Alg-PLGA MP, Alg-PLLA MP and CaAlg beads are shown below in **Figure 4.2.5**.

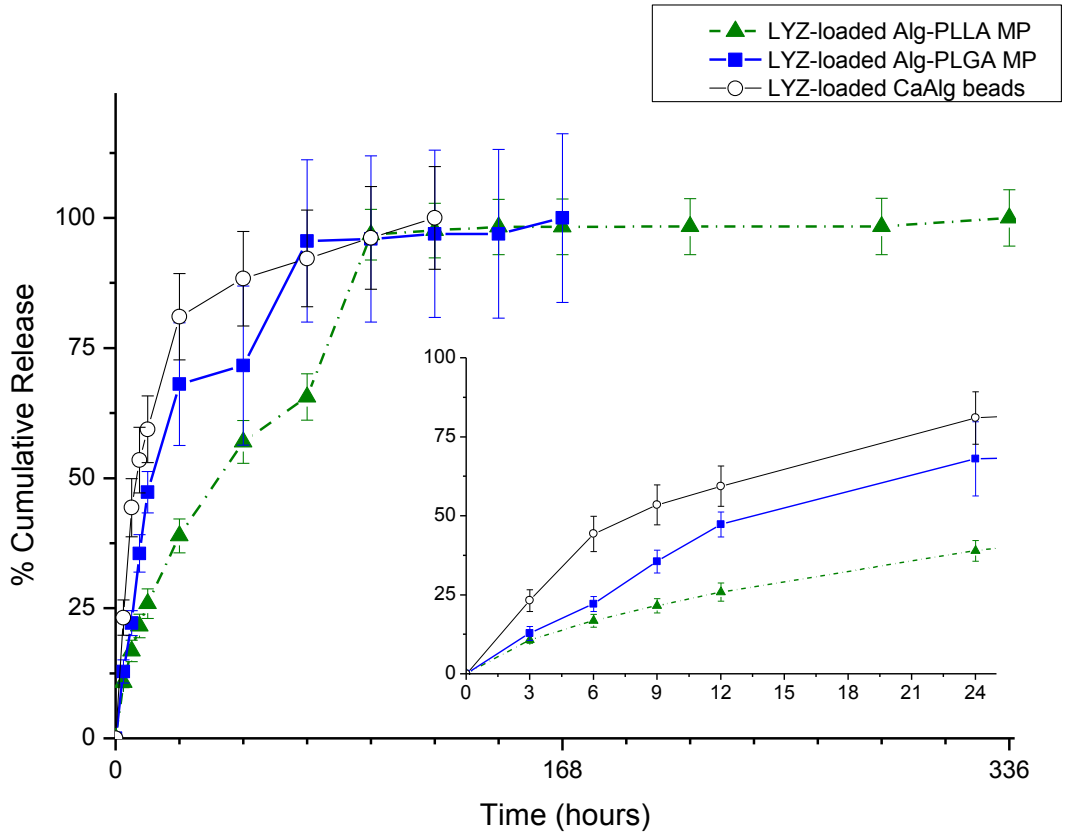

Figure 4.2.5: Release comparison between LYZ-loaded Alg Polyesteric MP and CaAlg beads across 2 weeks (main plot), close-up of release profile on the first 24 hours (inset)

It is noted that Alg-PLGA MP and Alg-PLLA MP demonstrated a sustained release over one and two weeks respectively. This is in comparison to naked CaAlg beads where a burst release of over 75% was observed within the first day. This difference in release is expected due to the hydrophobic shell of the Alg-PLGA MP protecting the CaAlg gel core, as compared to naked CaAlg beads. In addition, it is also observed that Alg-PLLA MP had a reduced burst release when compared to Alg-PLGA MP in the first 24 hours. This was expected due to the relative semi-crystallinity and hydrophobic nature of PLLA

as compared to PLGA, as previously seen in the release of MCA-loaded Alg-PLGA and Alg-PLLA MP.

4.2.1.3 Bioactivity of lysozyme released from LYZ-loaded Alg-Polyesteric MP

The bioactivity of released lysozyme was verified using the Micrococcus Lysodeikticus (ML) lysing assay. The change in turbidity of the ML suspension due to lysis, with the addition of the release aliquots was compared to a native lysozyme control and denatured lysozyme controls.

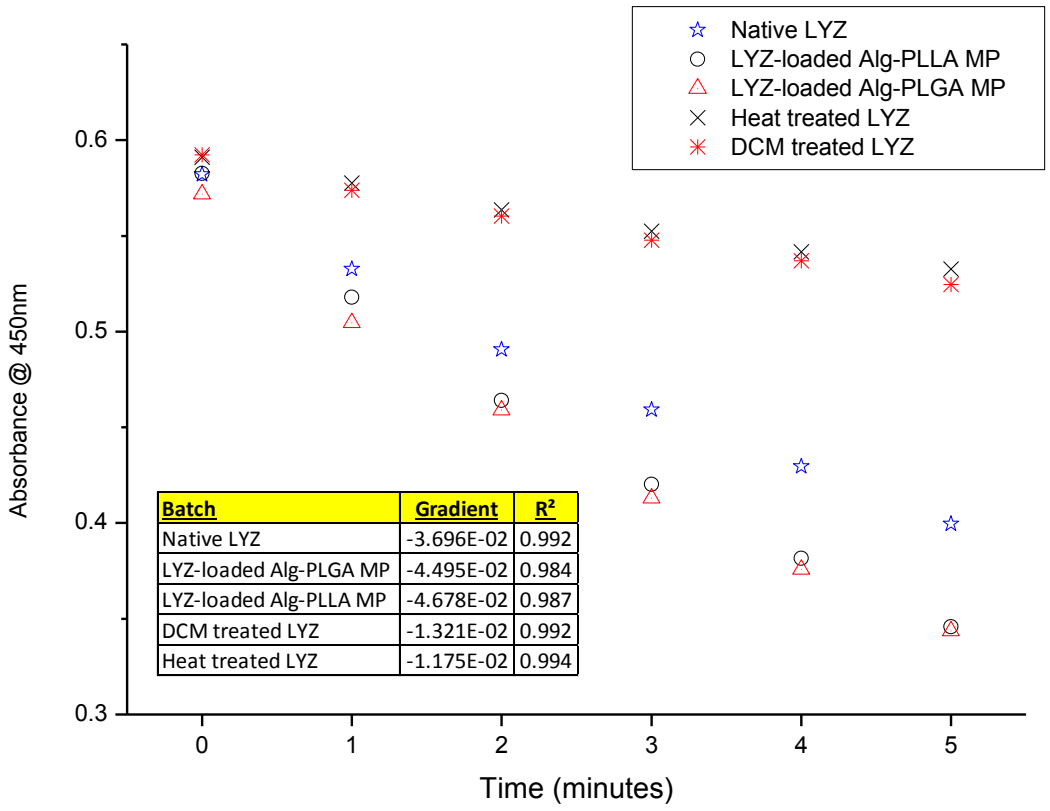

Figure 4.2.6: Plot of absorbance at 450nm against time, describing change of turbidity after addition of lysozyme to ML cells; inset table indicating the gradient of plots and respective R^2 values

The rate of change in turbidity (i.e. gradient of plots) of release aliquots from Alg-PLGA MP was observed to be similar to the native lysozyme control; whereas lysozyme denatured by either heat or vortexing in DCM, exhibited a slower change in turbidity. It

is hence inferred from here that the bioactivity of lysozyme encapsulated after release is preserved, as compared to the negative controls used to establish bioactivity.

4.2.2 BSA-loaded Alg-Polyesteric MP

4.2.2.1 Cross-section morphology of microparticles fabricated.

The SEM images of cross-sectioned BSA-loaded Alg-PLGA MP fabricated are shown below in **Figure 4.2.7**. It was observed that microparticles fabricated have a CaAlg core located within a PLGA matrix, similar to fabricated LYZ-loaded Alg-PLGA MP microparticles. Likewise, when BSA-loaded Alg-PLLA MP was fabricated, a similar structure was obtained, as shown in **Figure 4.2.8**.

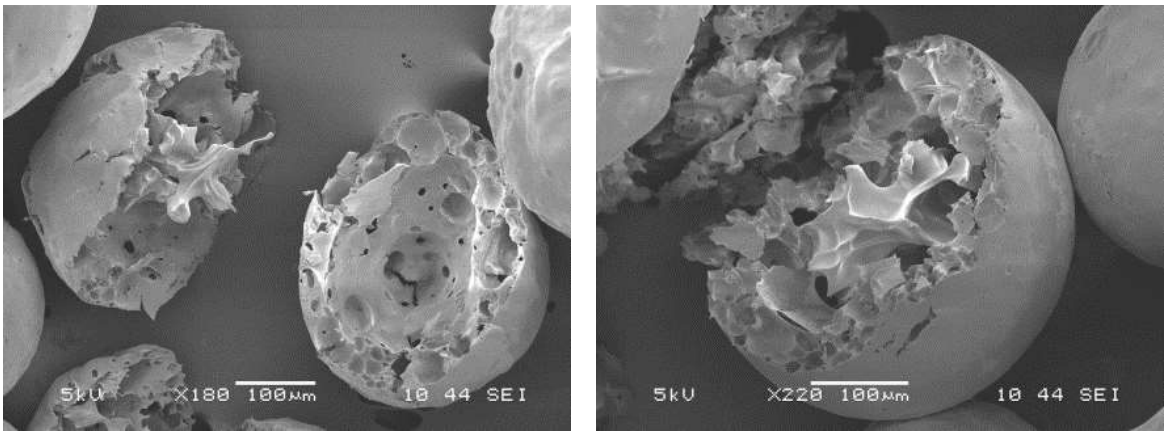

Figure 4.2.7: SEM images showing cross-section of BSA-loaded Alg-PLGA MP

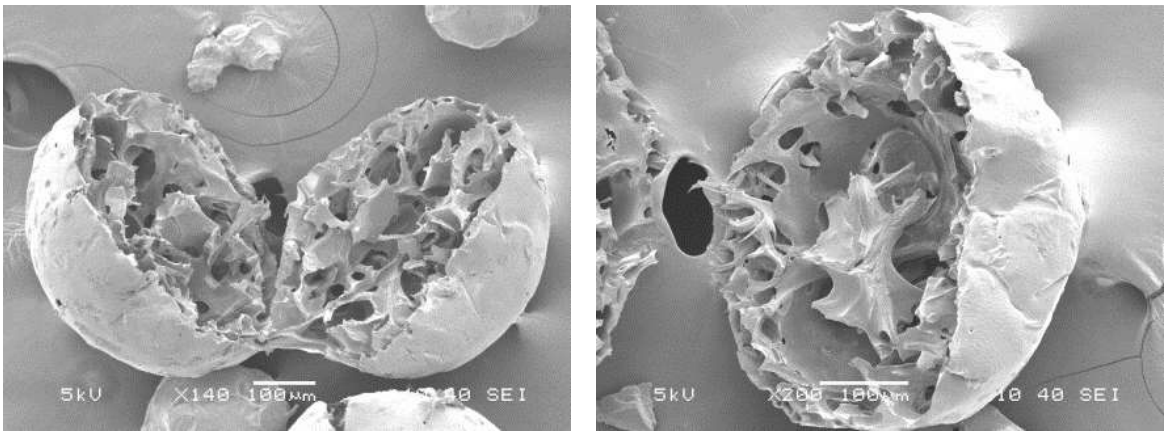

Figure 4.2.8: SEM images showing cross-section of BSA-loaded Alg-PLLA MP

In **Figure 4.2.9**, EDX mapping indicates that the central portion of the BSA-loaded Alg-PLGA MP was calcium rich, indicating that the core consists of CaAlg gel. Similarly, the presence of calcium was also found to be localized in the center of BSA-loaded Alg-PLLA MP, as confirmed by EDX mapping (**Figure 4.2.10)**.

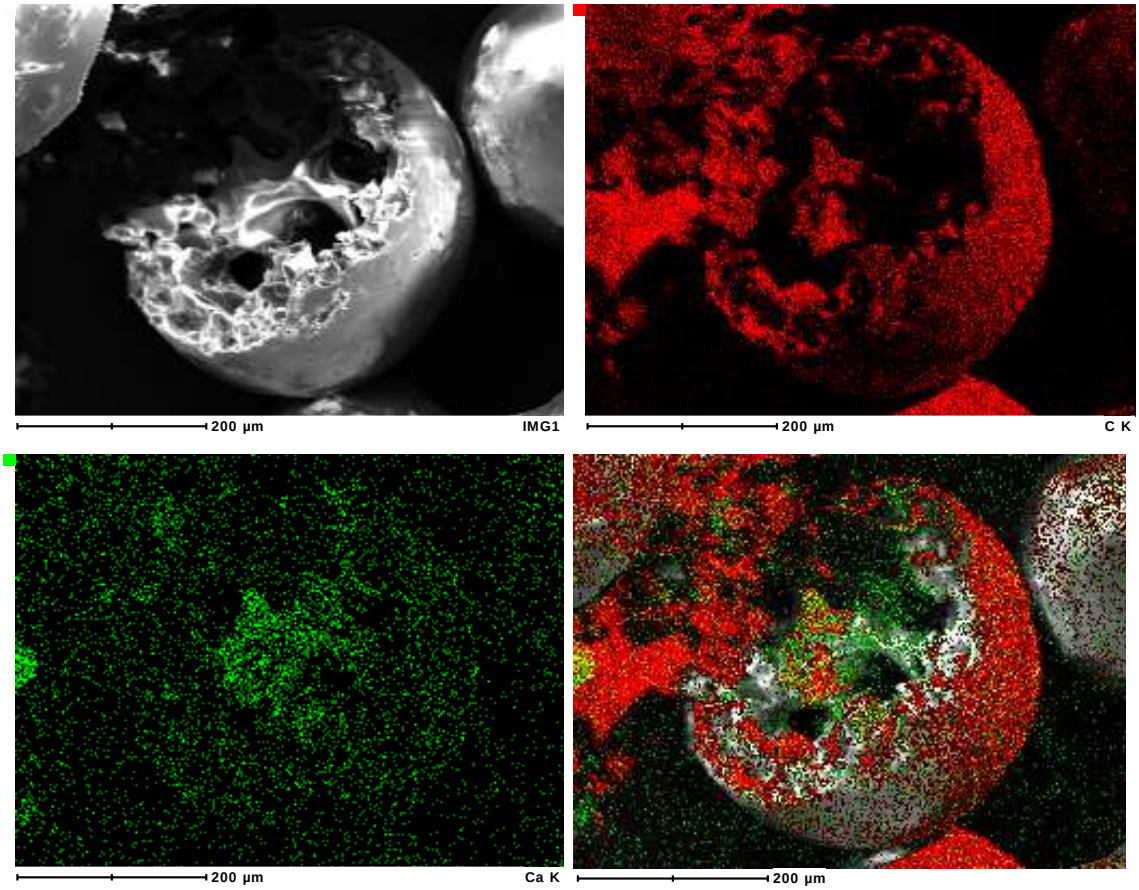

Figure 4.2.9: SEM/EDX map of a BSA-loaded Alg-PLGA MP
(red represents location of carbon, green represents location of calcium)

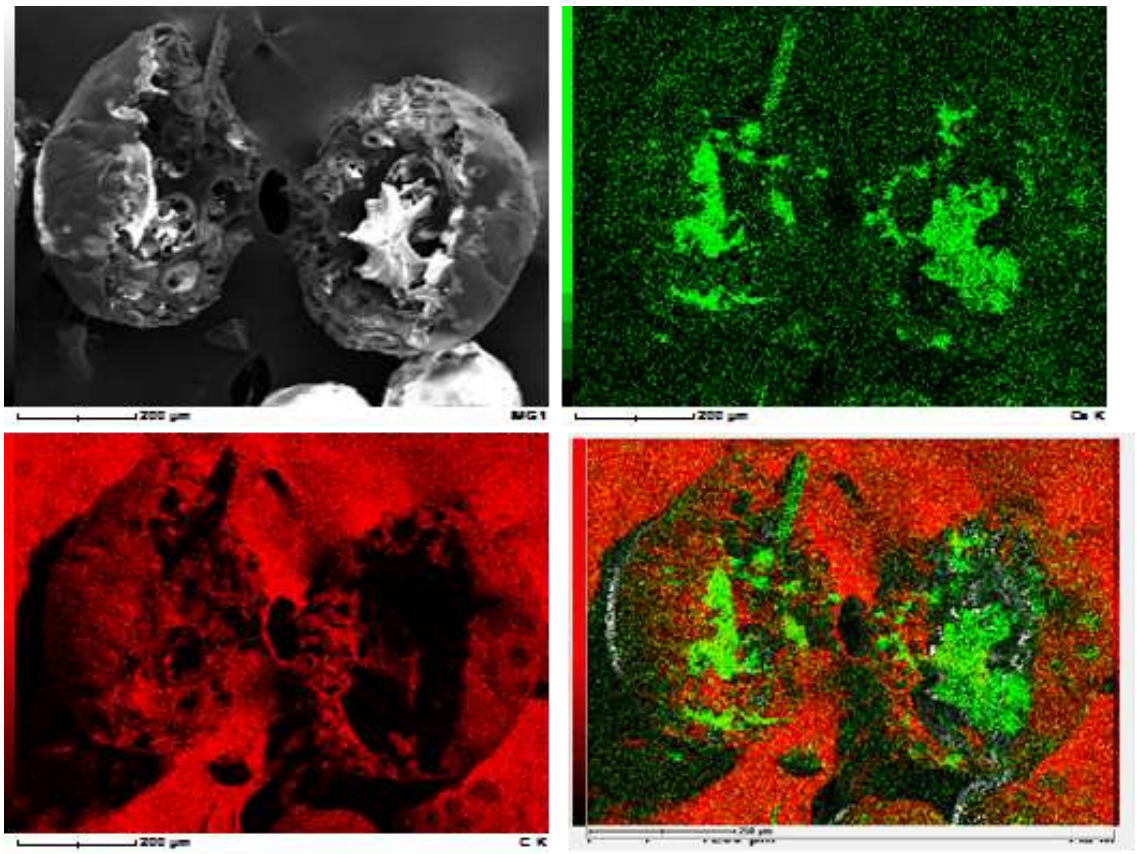

Figure 4.2.10: SEM/EDX map of a BSA-loaded Alg-PLLA MP
(red represents location of carbon, green represents location of calcium)

4.2.2.2 Encapsulation efficiency and release from BSA-loaded Alg-Polyesteric MP

The loading efficiencies were compared between BSA-loaded Alg-Polyesteric MP and neat polyesteric microparticles (**Table 4.2.2**.)

BSA Encapsulation Efficiency (%)		
Shell Polymer / Microparticle Type	**Monolithic matrix**	**Alginate core + Polymeric shell**
PLGA	110.06 ± 3.17	64.19 ± 9.87
PLLA	67.14 ± 8.99	94.34 ± 3.31

Table 4.2.2: Loading efficiency of BSA-loaded Alg-Polyesteric MP, compared to neat microparticles

It is observed here that microparticles fabricated with PLGA had a better EE compared to

PLLA based microparticles. This is observed for LYZ-loaded microparticles previously, and is attributed to the hydrophilic character of PLGA. The resultant poorer encapsulation efficiency for BSA-loaded Alg-PLGA MP could be due to the osmotic pressure differences, causing increased leaching during fabrication. It is noted however, that BSA-loaded Alg-PLLA MP had better EE compared to neat PLLA microparticles. This is attributed to the larger molecular weight of BSA retained within the W_{int} droplet with alginate inside, and the resultant reduced likelihood to partition into a PLLA/DCM layer during fabrication.

The release of BSA from BSA-loaded CaAlg beads, Alg-PLGA MP and Alg-PLLA MP are shown below in **Figure 4.2.11**. It is observed that BSA-loaded CaAlg beads had a large burst release of BSA within the first day and completed release within a week; whereas BSA loaded Alg-PLGA MP and Alg-PLLA MP continued to release the encapsulated BSA over 2 and 5 weeks respectively. This indicates the encapsulated shell of the polymer limits the release by acting as a barrier between the alginate gel component and the release medium, as previously reported for MCA-loaded Alg-Polyesteric particles observed.

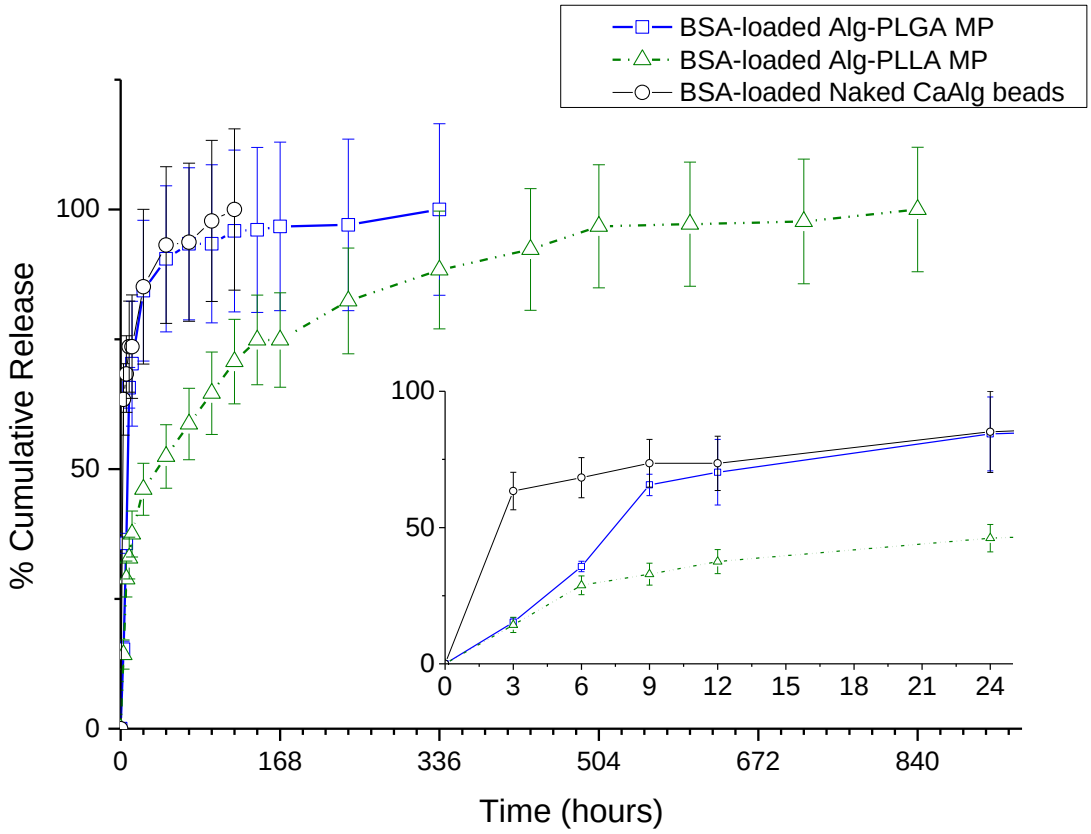

Figure 4.2.11: Release comparison of BSA-loaded Alginate beads vs. Alg-Polyesteric MP across 5 weeks (main plot), close-up of release profile on the first 24 hours (inset)

It was also shown that the BSA release from Alg-PLLA MP was noticeably slower than Alg-PLGA MP, both during the first 24 hours and over the entire period of release. This is explained by the different polymer type used, in that the more hydrophobic and semi-crystalline PLLA had a retarded release compared to amorphous PLGA. This affirms that the choice of polymer used will limit the release by the nature of the polymer shell used to encapsulate the CaAlg gel core.

4.2.2.3 Preservation of BSA structure after release

Release aliquots from the BSA-loaded Alg-PLGA MP and Alg-PLLA MP were assayed using circular dichronism (CD) and SDS-PAGE to observe for any major changes to the protein structure after release. The CD spectra of released BSA from Alg-PLGA MP and Alg-PLLA MP were compared with native BSA below in **Figure 4.2.12**:

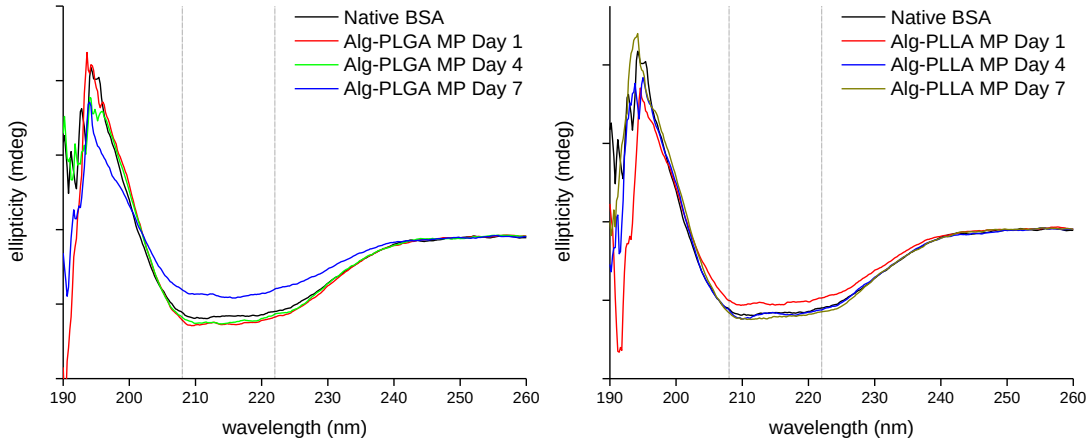

Figure 4.2.12: CD spectra for release aliquots for BSA-loaded Alg-PLGA MP and Alg-PLLA MP

Native BSA control and the released BSA at day 1, 4 and 7 of release from microparticles were observed to have the same negative maxima at 208 nm and 222 nm, indicating the α-helix structure present in BSA [72]. Given the similarity in ellipticity when comparing between native BSA and the released BSA, it can be presumed that the secondary structure of the BSA released from Alg-PLGA MP is generally preserved and did not undergo major alteration due to the fabrication or release conditions. Likewise, the release of BSA from Alg-PLLA MP at day 1, 4 and 7 exhibited the same ellipticity, also indicating the secondary structure of BSA were also mostly maintained post release. It is noted though, that the signals detected were low due to a lower concentration of BSA released.

The SDS-PAGE of release aliquots were also compared with a native BSA control and an acid hydrolyzed BSA control, as shown below in **Figure 4.2.13**:

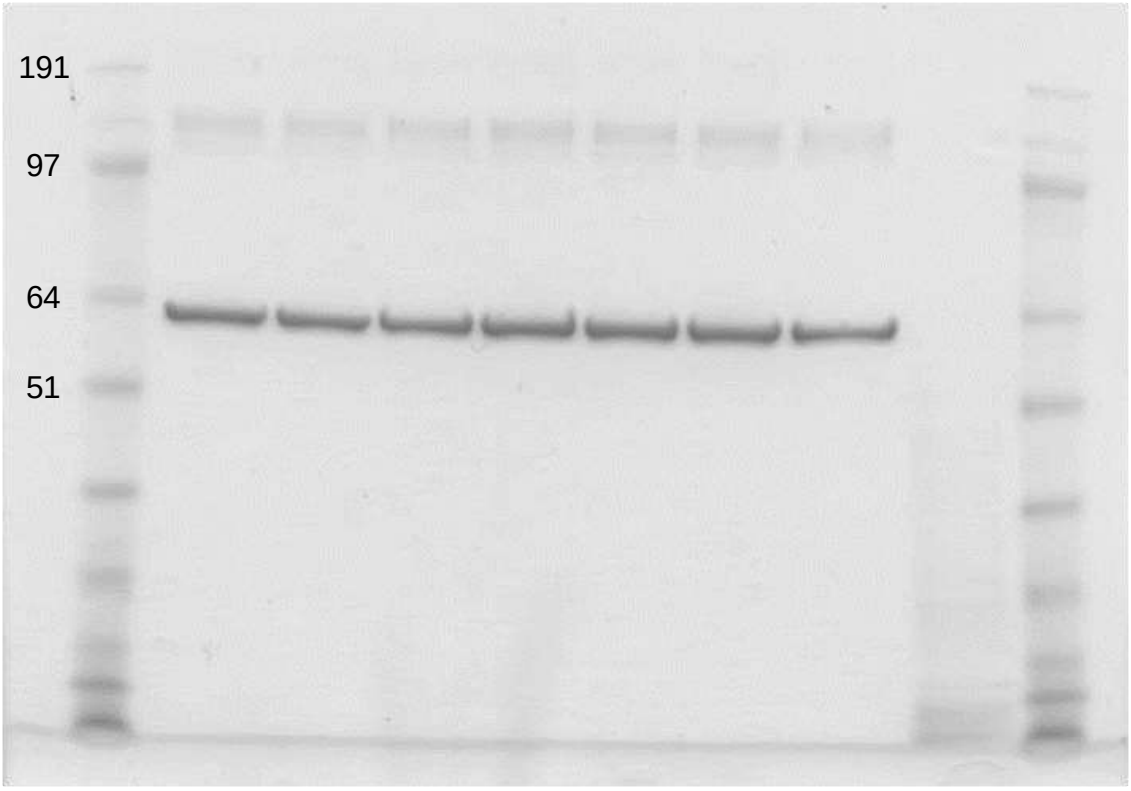

Figure 4.2.13: SDS-PAGE image of release aliquots with Native BSA and degraded BSA (From left, Alg-PLGA MP Day 1, 4, 7; Alg-PLLA MP Day 1, 4, 7; Native BSA control, acid hydrolysed BSA, flanked by molecular weight ladder on left and right of gel)

The bands seen for day 1, 4, and 7 from the release aliquots are observed to be similar with the native BSA control on the third last lane. Also, there is no observable fragmentation of proteins in the release aliquots observed on the gel electrophoresis below the major band of BSA (66.4 KDa). From this, it is inferred that the released BSA from particles did not undergo structural degradation of the protein backbone.

4.2.3 Variation of fabrication conditions for protein-loaded microparticles

In this section, the variation of conditions fabricating BSA-loaded Alg-Polyesteric MP is discussed, on the effect on particulate formation and the release behavior. This includes the variation of the [$CaC1_2$] concentration in the W_{ext} phase, and the volume of W_{ext} phase used.

4.2.3.1 Variation of [$CaCl_2$] in the external water phase

The concentration of $CaCl_2$ used in the external phase was varied during fabrication, and it was observed that microparticles fabricated had variation in size and presence of ruptured particles. Among the different concentration used, microparticles fabricated with 50 mM [$CaCl_2$] were observed to have minimal size variation and ruptured microparticles, when compared to other concentrations (**Figure 4.2.14**).

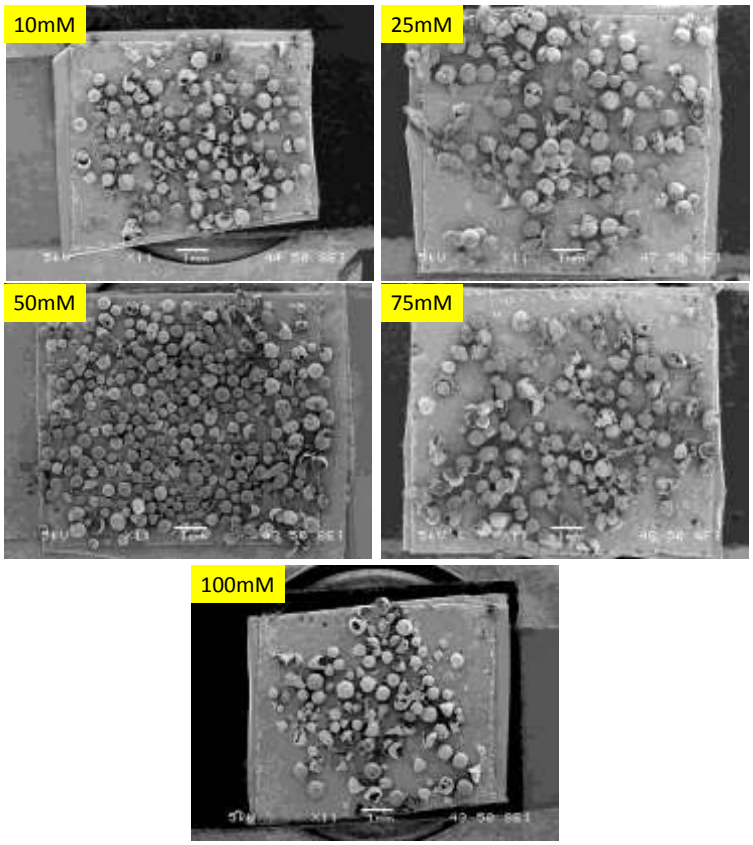

Figure 4.2.14: Overview of microparticles fabricated with different [$CaCl_2$] in the external phase

It was also observed that microparticles fabricated with concentrations above or below 50 mM had more surface features, such as wrinkles, pores and "pimples" (**Figure 4.2.15**).

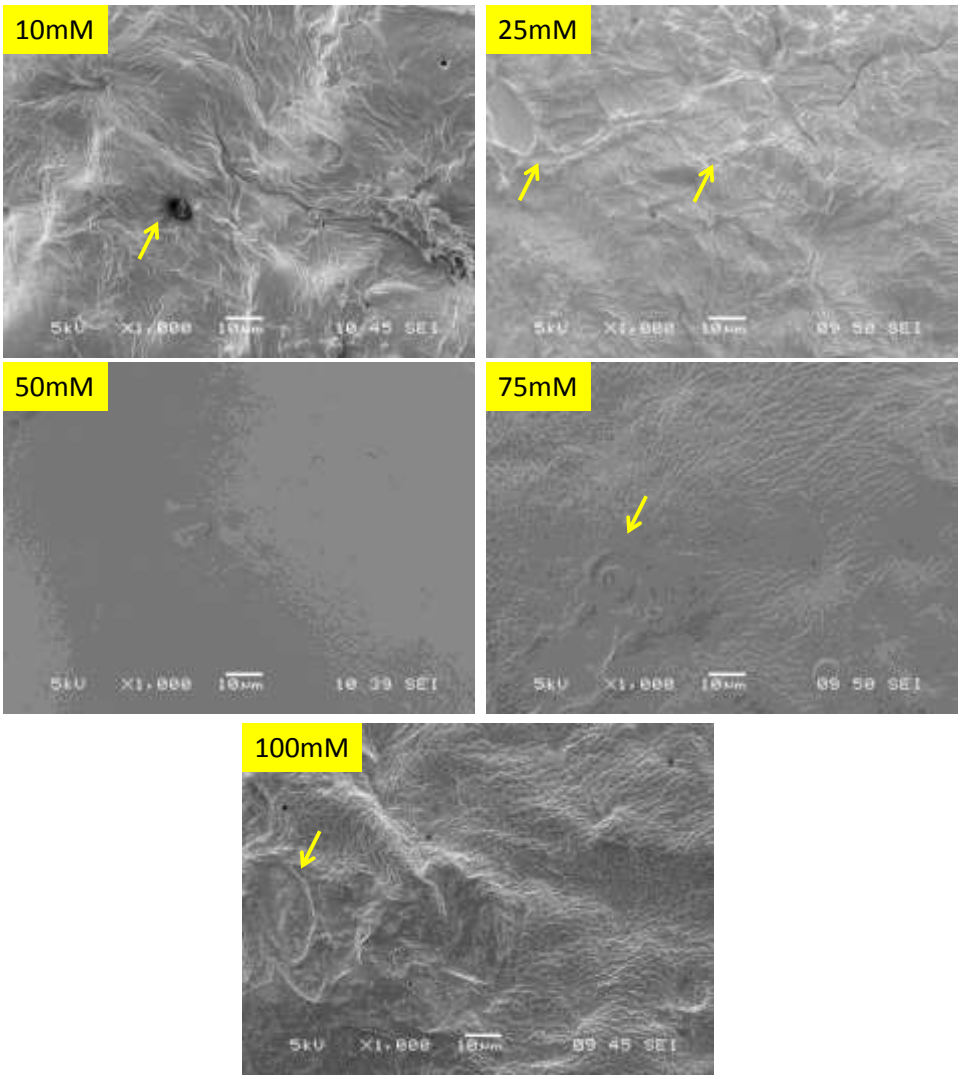

Figure 4.2.15: Overview of microparticle surfaces fabricated with different [$CaCl_2$] in the external phase

In terms of release, particles fabricated with [$CaCl_2$] = 50 mM or 75 mM demonstrated a more sustained release with a reduced burst. This is as opposed to microparticles fabricated with [$CaCl_2$] of 25 mM, 75 mM and 100 mM, which demonstrated a larger burst release compared to the rest (**Figure 4.2.16**).

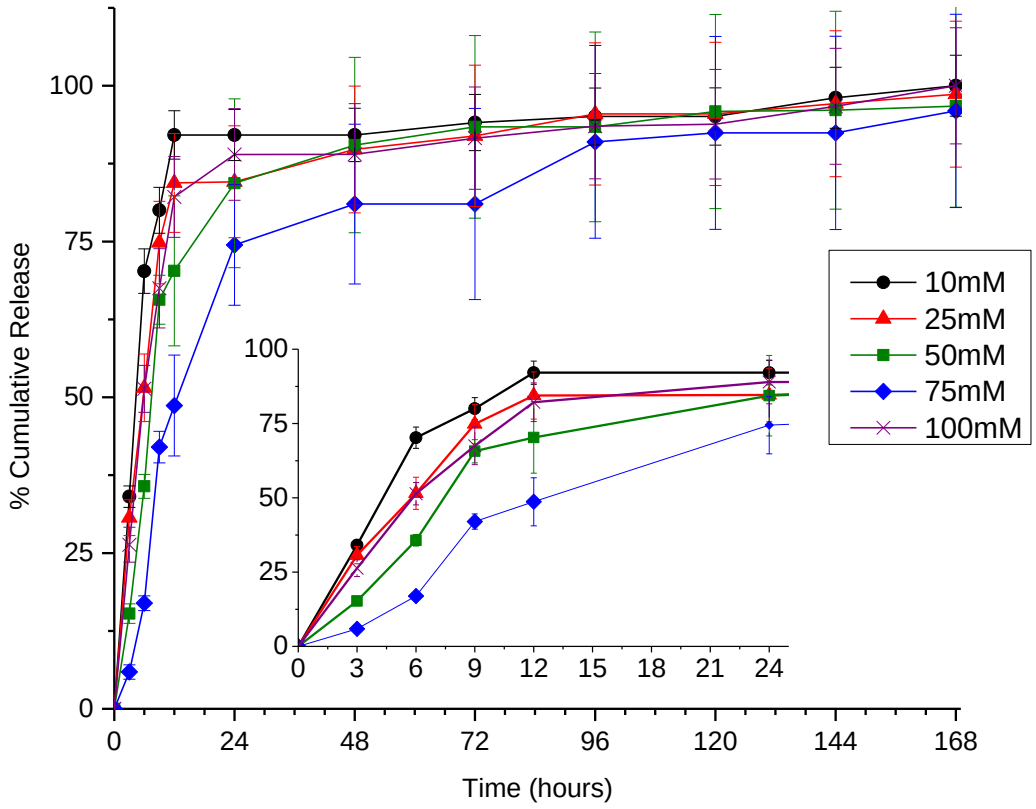

Figure 4.2.16: Release of BSA from microparticles fabricated with different [$CaCl_2$] in the external phase across 1 week (main plot), close-up of release profile on the first 24 hours (inset)

The difference in release behavior was expected to be due to ruptured particles and surface artifacts, such as the pores formed on the microparticle surface during fabrication, which were observed with microparticles fabricated with concentrations above or below 50 mM.

This difference in surface topography and the particle size distribution with the variation of [$CaCl_2$] in the external phase observed could be explained to be due to the presence of an osmotic pressure gradient between the aqueous phases of the double emulsion during fabrication. If a hypotonic or hypertonic situation occurs, where a lower or higher solute

concentration is present in the W_{ext} phase as compared to the W_{int} phase respectively [58], this causes an osmotic pressure difference, resulting in water movement via osmosis across the semi-permeable oil membrane. This may then result in an uneven size distribution of particles, due to varied uptake of water between different w/O double emulsion droplets. The movement of water either by bulk or osmosis across the oil membrane may also cause pores, water channels and particulate rupture to occur [7]. This may then explain for the burst release observed for extreme concentrations away from 50 mM. Likewise for the surface wrinkling observed could be due to increased osmotic pressure forces acting on the double emulsion droplet surface at the point of hardening, resulting in an uneven surface or distortion of the oil membrane.

4.2.3.2 Variation in volume of external water phase

Figure 4.2.17 shows the representative SEM images of surface details of microparticles fabricated with different volumes of the W_{ext} phase. It is observed that when 150 ml or 250 ml of W_{ext} phase is used, the fabricated microparticle surfaces appeared to be covered with holes or patches of coating. These patches are not observed on particles fabricated with a decreased volume of W_{ext} phase such as 75 ml or 100 ml.

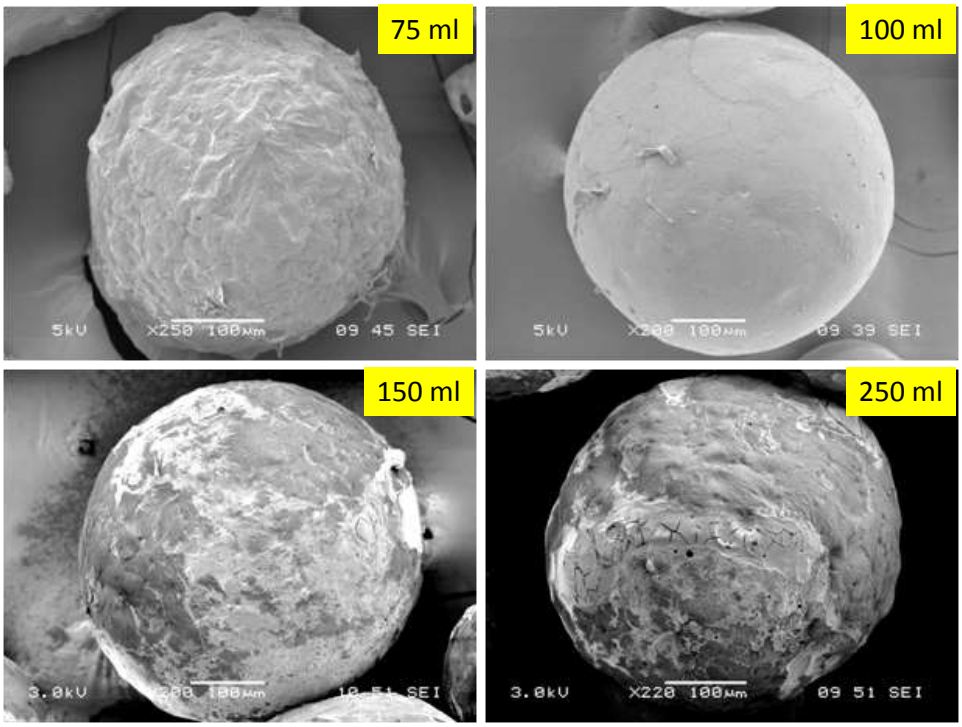

Figure 4.2.17: Representative SEM images showing surfaces of particles of batches fabricated with different volume of external water phase.

These patches were prone to charging during electron microscopy scans, and were identified to be calcium rich when an EDX was performed on these regions, implying the localization of CaAlg in these areas (**Figure 4.2.18 and 4.2.19**).

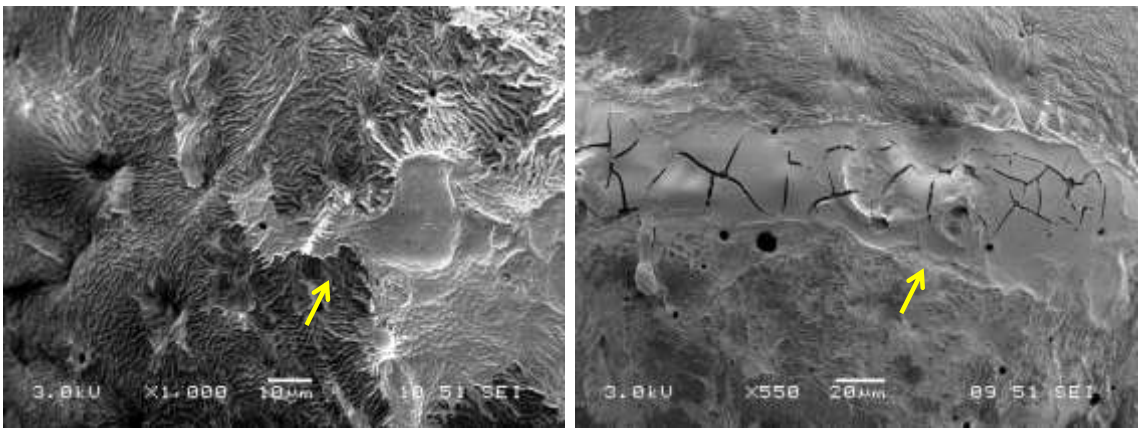

Figure 4.2.18: Close up SEM images showing surfaces of microparticle batches fabricated with 150ml (left) and 250 ml (right) of W_{ext} phase

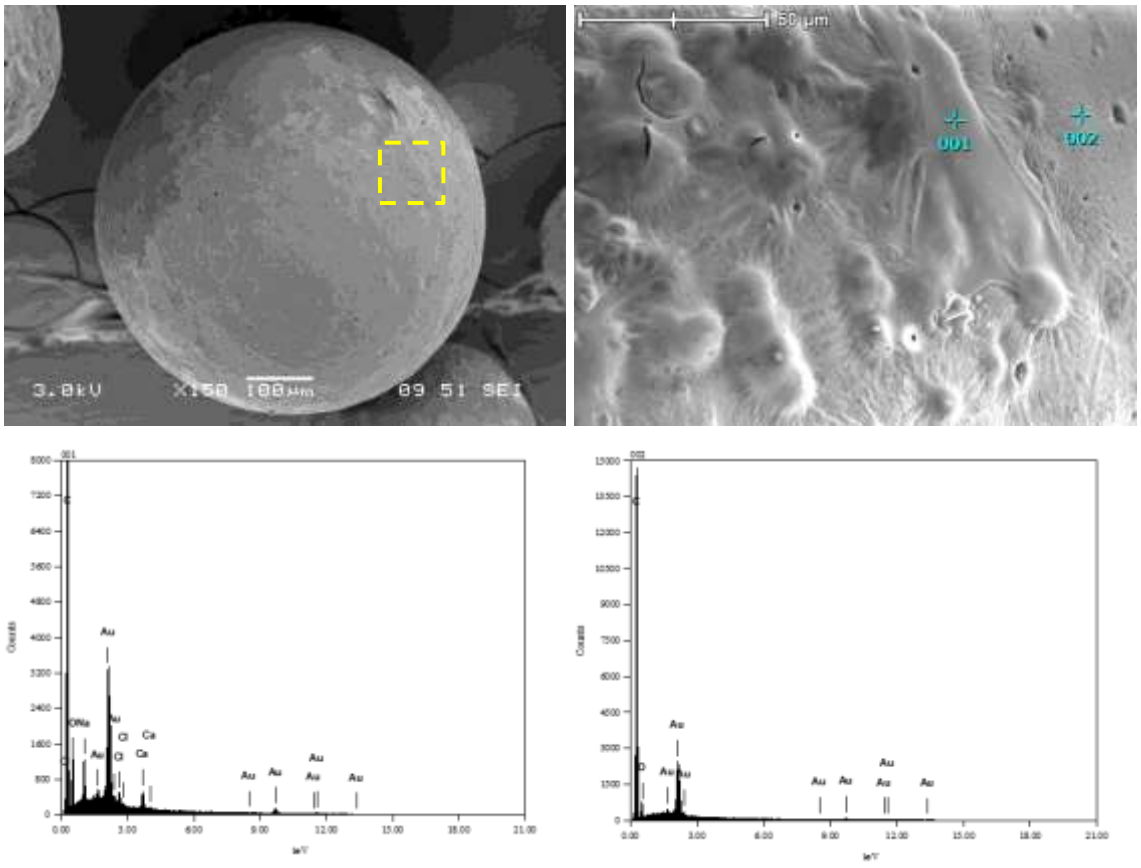

Figure 4.2.19: SEM image of a microparticle fabricated with 250 ml of external phase, with close up of the regions and EDX on two regions covered and uncovered with alginate patches.

Figure 4.2.20 shows images of the microparticles formed. The microparticles were also measured and counted in bin intervals, shown in **Figure 4.2.21**. It is likewise observed, that microparticles fabricated with 100 ml of external phase had a narrower particulate distribution compared to the other volumes used. Also, with a larger volume of W_{ext} phase (250 ml) used, the particles fabricated appeared to be smaller in size.

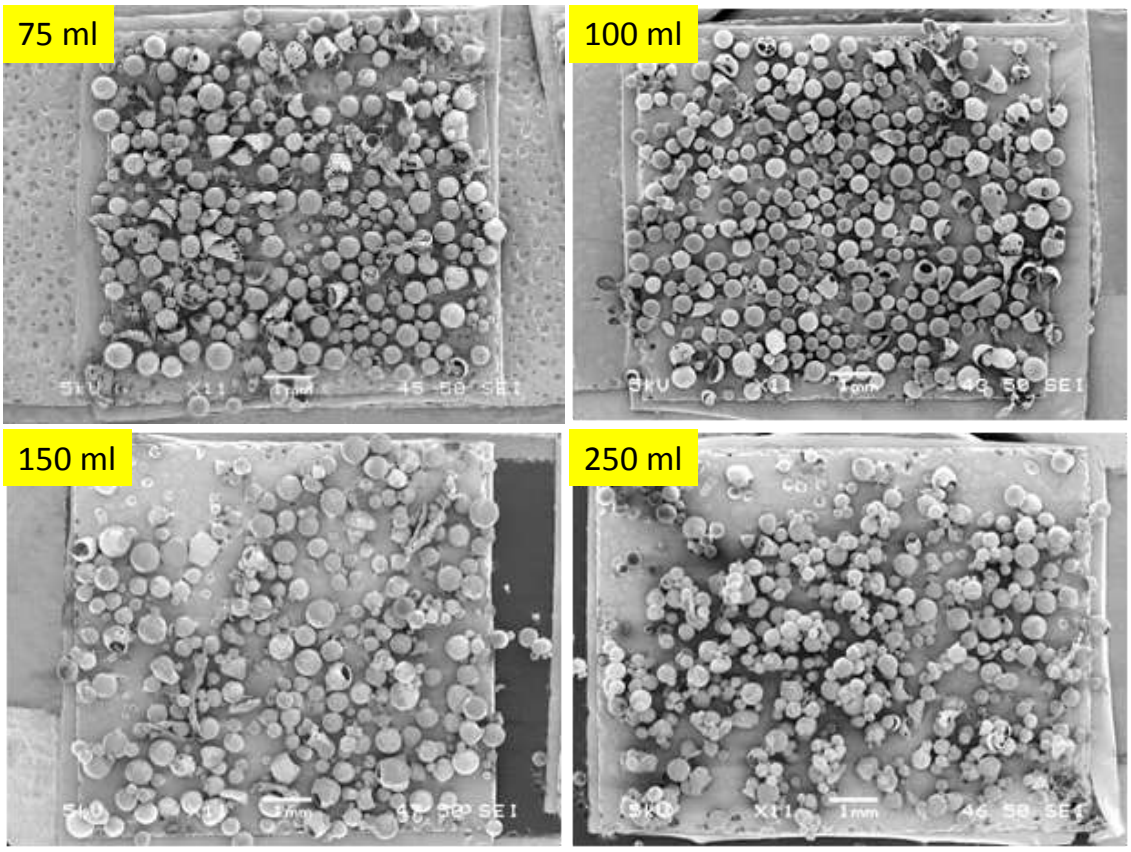

Figure 4.2.20: SEM images showing size distribution of particles of batches fabricated with different amount of external water phase.

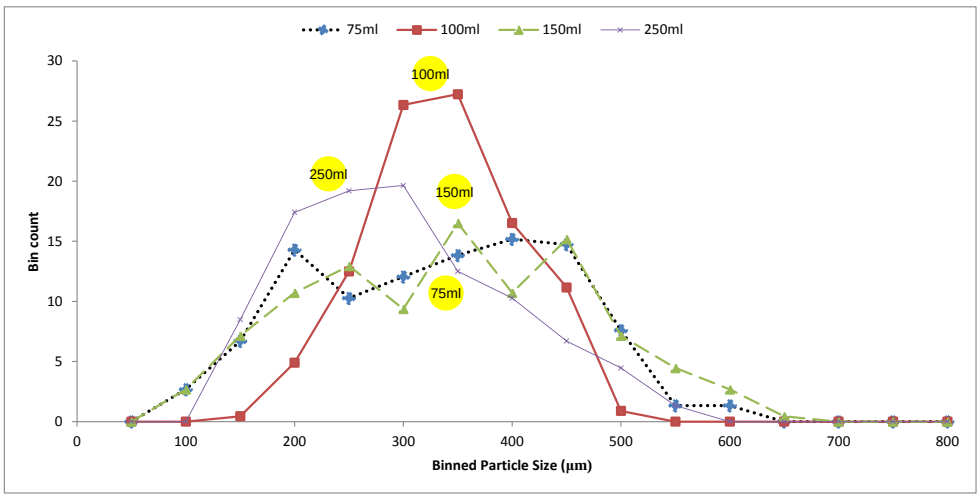

Figure 4.2.21: Plot showing particulate count vs. particulate size binned at 50um intervals for different volumes of W_{ext} fabricated.

The release of BSA from the microparticles fabricated is compared as shown in **Figure 4.2.22**. Microparticles fabricated using larger volume of W_{ext} phase demonstrated a larger burst release, compared to microparticles fabricated with a smaller volume of W_{ext} phase.

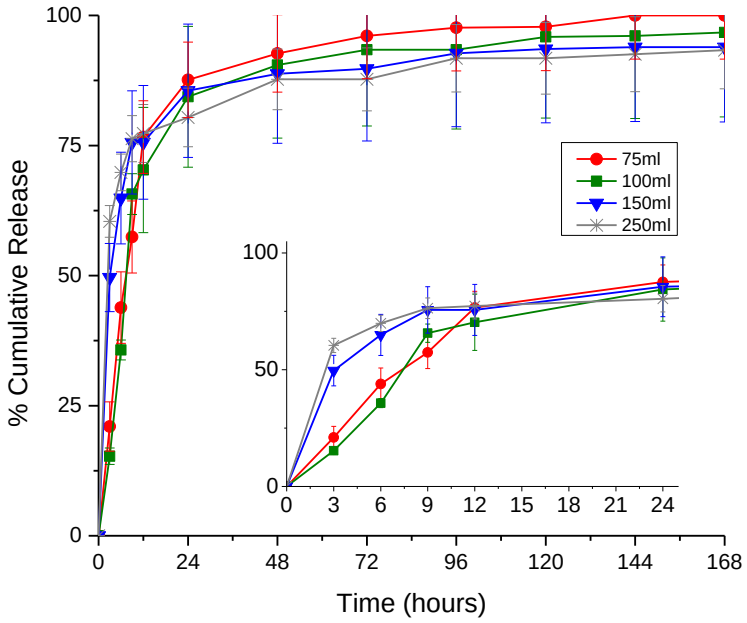

Figure 4.2.22: Release comparison of microparticles fabricated with a different volume of W_{ext} across 1 week (main plot), close-up of release profile on the first 24 hours (inset)

The observation made in the change in particulate morphology and release behavior, could be due to a change in polymer precipitation rate, with a difference in the W_{ext} volume used. With an increased volume of external phase, the precipitation rate increases with a higher DCM solvent concentration gradient between the two aqueous phases [30]. A fast rate of hardening resulting from a large volume of external W_{ext} phase would then harden and freeze the state of a w/O emulsion droplet immediately.

Since a double emulsion is not expected to be stable, the tendency for the W_{int} droplets to coalesce and form a larger W_{int} droplet in the w/O droplet, is highly probable to reduce the surface energy of the double emulsion [56]. With a fast hardening rate due to a larger volume of W_{ext} phase, this may result in insufficient time for the smaller W_{int} droplets to move away from the DCM/PLGA membrane and regroup at the center of the w/O emulsion droplet. This may then explain why CaAlg was observed on the surface of the particles when a larger volume of W_{ext} phase was used, causing the larger burst release observed. Conversely, if the W_{int} phase were allowed to coalesce at the core of the w/O droplet, instead of the surface before hardening, this would reduce the burst effect when lower volume of W_{ext} phase is used.

The smaller sized microparticles observed with a larger volume of W_{ext} phase used, could be also due to the fast hardening of microparticles during solvent evaporation, preventing further osmosis of water through the PLGA/DCM layer into the microparticles. On the contrary, if microparticles do not harden immediately, this may allow an increase influx of water into w/O droplets, causing the swelling of the w/O droplets before hardening due

to the presence of osmotic pressure. This could then explain for the larger sized microparticles and a wider size distribution observed for lower volumes of W_{ext} phase used.

4.2.4 Discussion

4.2.4.1 Fabrication of protein-loaded microparticles and bioactivity post release

In this study, batches of LYZ-loaded and BSA-loaded Alg-Polyesteric MP were fabricated to examine the effect of protein loading on particulate formation, release behavior, and preservation of the protein structure post-release. Microparticles were fabricated by first dissolving NaAlg within a protein solution to form a W_{int} phase, before emulsification into a PLGA/DCM solution, then into a W_{ext} phase containing PVA and $CaCl_2$. Concurrent solvent evaporation and alginate gelation by calcium ions produced microparticles similar to MCA-loaded microparticles, where the cross-section of microparticles had CaAlg gel material dispersed within a PLGA matrix. Variants of different polymer shell of Alg-Polyesteric MP were also fabricated by just varying the type polymer dissolved in the solvent used for the oil phase.

It was observed that for protein-loaded microparticles, the EE was not as high as was expected, or was seen in MCA-loaded microparticles. This was attributed to the amphiphilic nature of proteins encapsulated, and was expected to differ with higher molecular weight of proteins encapsulated.

In terms of release, Alg-Polyesteric MP were shown to have a reduced burst release compared to naked CaAlg beads, observed in both BSA-loaded or LYZ-loaded Alg-Polysteric MP. This indicates that an additional polymer shell could control and slow down the release of encapsulant from the CaAlg core. The use of different polymers as the shell of the microparticle fabricated also changes the release rate, depending on the

type of polymer used. With a more slowly degrading or a more hydrophobic polymer, the rate of release can be reduced. This indicates that release rates can be tailored by polymer choice. This could extend to beyond the polymers used for this study, including those of higher molecular weight or other non-polyester based biopolymers.

Preservation of protein structure is also evident after release: For BSA released from microparticles, SDS-PAGE did not show any fragmentation of the BSA released; the CD spectra of release aliquots also showed no major change in secondary structure of BSA after release as well. In the case of lysozyme, the use of the Micrococcus Lysodeikticus lysing assay indicates the preservation of bioactivity and lysing ability of lysozyme post release. Hence, this pointed to ability of the Alg-Polyesteric MP to preserve the bioactivity of encapsulated biomolecules after their release.

4.2.4.2 Changes in fabrication conditions in the external water phase

Two of the fabrication variables examined was the change in the [$CaCl_2$] of the W_{ext} phase, and also the volume of the Wext used. It is noted that $CaCl_2$ in the W_{ext} phase, provided a source of Ca^{2+} ions for the gelation of NaAlg; whereas the volume of the W_{ext} phase controlled the solvent evaporation rate of the emulsion droplets formed.

When [$CaCl_2$] of the W_{ext} phase was varied between 10 mM and 100 mM, it is noted that concentrations away from the mid-point concentration 50 mM, resulted in fabricated particles with various forms of swelling and rupture or surface artifacts. This also subsequently affected the release sustainability for these concentrations. Given the

DCM/PLGA polymer solution layer can be perceived as a semi-permeable membrane, between the water phases in a double emulsion [58], a change in [$CaCl_2$] alters the osmotic pressure resultant in the W_{ext} phase. It is then expected that the osmotic pressure gradient changes with variance in [$CaCl_2$]. Hence, any resultant extreme imbalance in osmotic pressure gradient may then cause destabilization of the double emulsion, due to large forces acting on the PLGA/DCM solvent layer separating the two water phases. As an outcome, surface artifacts and rupture of particles is evident on these microparticles fabricated as a result of a large osmotic pressure gradient, subsequently affecting release. This likewise suggests that the 50 mM [$CaCl_2$], can be used as a central reference point for minimal osmotic pressure mismatch across the DCM/PLGA layer,

When the W_{ext} phase volume was varied between 75 ml and 250 ml, it is observed that when a much larger volume such as 150 ml or 250 ml used caused the formation of cracks and patches of CaAlg on the microparticle surface. This appears to account for the burst release behavior, which was otherwise not observed for a lower volume of W_{ext} phase used. In addition, the microparticle surface of microparticles fabricated with lower volumes such as 75 ml and 100 ml, did not have the CaAlg patches and cracks on the particulate surface. Since a large volume of the W_{ext} phase affects the DCM solvent extraction rate, this may have accelerated the hardening and precipitation rate of the DCM/PLGA layer.

It is also noted that since double emulsions are inherently instable, the coalescing of the W_{int} droplets reduces surface energy at the interfaces as part of destabilization [56].

Hence, it is then postulated that if the W_{int} droplets is not allowed sufficient time to move inward towards the core and coalesce in the center of the w/O emulsion droplet prior to hardening, the resultant W_{int} droplets containing NaAlg would remain on the surface of the hardened w/O droplet, causing gelation to occur on the surface instead of diffusing through the DCM/PLGA membrane layer. This would result in the surface defects seen in microparticles fabricated with large volume of W_{ext} phase used; which was thus otherwise avoided with a lower volume of W_{ext} phase.

Also, smaller sized microparticles were observed with a larger volume of W_{ext} phase used and a lower volume of W_{ext} phase used resulted in larger sized particles and a wider size distribution observed. Given a faster precipitation rate with more external water phase volume, it is also inferred that the fast hardening of the PLGA/DCM layer prevents the osmosis of water into the w/O droplet. This could hence explain the larger sized particle and a wider size distribution observed for lower volumes of water used. As a result, it is possible here that the precipitation rate of the w/O droplet here limits the diffusion of contents across the PLGA/DCM layer.

Hence, in terms of particulate formation mechanics, it can be conceived that the below processes that would occur during fabrication, based on the observations made:

- First the w/O/W double emulsion forms, with an internal NaAlg dissolved W_{int} phase and a W_{ext} phase consisting of PVA surfactant and $CaCl_2$ as a gelling ion source. The oil phase, i.e. the PLGA/DCM polymer solution layer, separates both the aqueous phases, and acts as a semi-permeable membrane, allowing osmosis and diffusion to

occur. This layer also contains the Span80 surfactant for the stabilization of the w/O primary emulsion.

- As the emulsion forms, solvent evaporation initiates, by the partitioning of DCM solvent from the PLGA/DCM layer into the external phase, before escaping into air/water interface of the double emulsion.

- Concurrently during solvent evaporation, Ca^{2+} ions diffuses through the PLGA/DCM layer into w/O double emulsion droplet, to cause gelation of NaAlg in the W_{int} droplets, forming CaAlg as an end result.

- Dependent on the w/O droplet hardening rate,
    - The influx of Ca^{2+} ions into the w/O double emulsion droplet is expected to increase with the amount of time the PLGA/DCM layer remains semi-permeable, which correlates to the volume of W_{ext} phase employed for solvent evaporation. The amount of Ca^{2+} content in the gelated CaAlg then correlates to the volume of W_{ext} phase in use.
    - The location and morphology of the gelated CaAlg gel material within the cross-section of the microparticles formed, is also an indication of the state of the w/O emulsion droplet prior to hardening. i.e.
        - If small bits of CaAlg gel material are found dispersed within the PLGA matrix, the W_{int} droplets did not coalesce prior to particle hardening. On the converse, if a single CaAlg core is found within a shell, this

would indicate that the W_{int} droplets would have coalesced prior to gelation.

- Also, if CaAlg patches are found on the surface of particles, this would also indicate the lack of inward movement towards the core of the w/O droplet and lack of coalescence of W_{int} droplets, before the particle hardens.

- Dependent on the amount of water or other osmolytes moving through the PLGA/DCM layer, movement in bulk that is incomplete before the particles completely harden, would result in defects that will cause burst release, including the formation of surface cracks, CaAlg patches, pores or water channels.
- The permeability of the PLGA/DCM layer during the occurrence of the concurrent process of solvent evaporation and ionotropic gelation, and other release behavior, would also be highly dependent on the hardening rate of the PLGA/DCM layer during fabrication.

Hence it is put forward that the final microparticle cross-section, surface morphology or topography, is reflective of the double emulsion state at the point of complete particle hardening, and is representative of the frozen state of events at that point. This would be seen as a correlation of solvent extraction and polymer precipitation rate; effects of osmotic pressure; and double emulsion stability. The resultant of these events coming together, will also affect the release behavior of the microparticles fabricated. This implies that fabrication of the Alg-Polyesteric MP system requires care in maintaining emulsion stability during fabrication.

Chapter 5 Conclusion

In this work, a novel microparticulate DDS was developed, by fabricating microparticles with a CaAlg hydrogel core, encapsulated by biodegradable hydrophobic polyesteric shell. These microparticles were fabricated using a one-step technique, with concurrent ionotropic gelation and emulsion solvent evaporation processes. The polymer shell can be varied by the choosing a suitable polymer to be dissolved in the oil phase.

The inclusion of CaAlg within PLGA or PLLA was shown to improve loading efficiency when a model hydrophilic drug, MCA was encapsulated within Alg-Polyesteric MP and compared to neat polyesteric microparticles without CaAlg. The polymer shell performed as a physical barrier between the drug-loaded hydrogel core and the release medium, thus modulating the release rate, variable by the type of shell polymer of the fabricated Alg-Polyesteric MP.

Alg-Polyesteric MP loaded with model proteins BSA and lysozyme also showed a difference in release rates, when compared to naked CaAlg beads, and the release rates were dependent on the shell polymer used. The BSA released from the microparticles also showed that the secondary structure was maintained and fragmentation did not occur after fabrication and release, through the use of circular dichronism and SDS-PAGE. Lysozyme released from the microparticles was also shown to maintain bioactivity, as seen in lysing activity in the Micrococcus Lysodeikticus assay.

In terms of microparticle fabrication, it is observed that the formation of a CaAlg gel within a PLGA matrix requires the concurrent ionotropic gelation of the NaAlg in W_{int} droplets within the w/O double emulsion droplet to form CaAlg; and solvent evaporation to cause precipitation of the shell polymer. It is also put forward that the PLGA/DCM layer during fabrication act as a semi-permeable membrane during fabrication and is subject to osmotic pressure forces acting on from both aqueous phases. The permeability of the PLGA/DCM layer before hardening and bulk movement of solutes and water moving through this layer affects the fabrication process. It is hence inferred that in correlation of the PLGA/DCM layer permeability, the solvent extraction and polymer precipitation rate; osmotic pressure effects, double emulsion stability, affects the particulate fabrication in terms of the cross sectional morphology, surface morphology and also subsequently release behavior.

Hence, there is hope that this new particulate DDS would be valuable in areas such macromolecular delivery of peptides, proteins and vaccines. Consequently, these hydrogel-core hydrophobic-shell microparticles would permit the improvement in encapsulation and release of water soluble drugs, and also a friendly environment for protein encapsulation.

Chapter 6 Recommendations

Future works on the alginate-polymer microparticle system are proposed below, for the deeper understanding of the properties of this particulate drug delivery system. This is especially on the drug loading and release behavior of proteins, and the different fabrication parameters that affect the particle formation.

6.1 Alternative fabrication methods

Given that the microparticles are fabricated by a simple double emulsion method performed by mechanical agitation or stirring, the drop size of the emulsion formed is largely determined by these mechanical shear forces and can be difficult to control dependent on the state of the emulsion and the fabrication conditions involved. This ultimately affects the particle size and shape distribution. Also, the high shear forces involved in mechanical stirring may result in rupture of double emulsion droplets, which cannot be easily controlled during turbulent flow emulsification. For a better control of emulsion droplet size, templating methods to form the primary water and secondary w/O emulsion droplet can be explored. This includes the use of droplet extrusion methods through a fixed opening or cross emulsification employed in microfluidics, in order to achieve constant emulsion drop size for particulate fabrication consistency.

It is also noted that during the microparticle fabrication, NaAlg was gelated via external gelation from an external Ca^{2+} source. Since this method of gelation is reported to form hydrogels of varying gelation gradient [73], an internal gelation method is also proposed to achieve homogenous gelling, to examine any differences in gelling and release behavior. Such a gelling method would involve dispersing insoluble $CaCO_3$ and the

addition of δ-gluconolactone to gradually cross-link the gel before secondary emulsification. Ideally, this would reduce the osmotic pressure gradient resulting from the use of Ca^{2+} in the external water phase.

6.2 Further mechanistic studies on the particulate formation

Further mechanistic studies can be conducted for the fabrication of the Alg-Polyesteric MP core shell system for in depth examination of the processes occurring during emulsification, gelation and solvent extraction. This can include the use of tracking dyes and the use of in-situ microscopy to track changes in time lapse intervals. In this manner, any major changes in osmotic pressure and movement of double emulsion droplet can be tracked.

Characterization of gelation properties of the resultant CaAlg gel core formed, including the gelation density, is also proposed to be studied via energy-filtered transmission electron microscopy. This would allow location of calcium rich regions for the study of gelation kinetics.

6.3 Further protein loading work on Alg-Polyesteric MP

Encapsulation efficiency is a problem, in spite of the use of a hydrogel to encapsulate proteins. Since this could be an issue of osmotic pressure during emulsification, further experiments on the protein concentration and basal calculations for osmotic pressure exerted by the protein and alginate in solution need to be determined to examine its effect on the double emulsion formed.

Also, given that lower encapsulation efficiency was due to a lower retention of encapsulated molecules within the core of the double emulsion, it is proposed that additives can be used to improve retention. Such additives could include other types of surfactants such as ionic surfactants like CTAB to examine the effect of charged surfactants on the encapsulation efficiency. Also, viscosity thickening agents added to the W_{int} phase such as carrageenan, can be also added to promote retention of these molecules in the double emulsion. These additives could also be varied in concentration to explore their effect on the double emulsion and the resultant encapsulation efficiency.

In addition, given that BSA and lysozyme in this study are model proteins to begin with; true therapeutic performance should be assessed by the loading and release of therapeutic macromolecules, such as growth factors and the use of ELIZA assay to further affirm the bioactivity of these proteins loaded after release.

Chapter 7 References

[1] E. R. Balmayor, H. S. Azevedo, and R. L. Reis, "Controlled Delivery Systems: From Pharmaceuticals to Cells and Genes," *Pharmaceutical Research,* vol. 28, pp. 1241-1258, 2011.

[2] K. J. Whittleseya and L. D. Sheaab, "Delivery systems for small molecule drugs, proteins, and DNA: the neuroscience/biomaterial interface," *Experimental Neurology,* vol. 190, pp. 1-16, 2004.

[3] S. Vrignaudabc, J.-P. Benoitabcd, and P. Saulnierab, "Strategies for the nanoencapsulation of hydrophilic molecules in polymer-based nanoparticles," *Biomaterials,* vol. 32, pp. 8593-8604, 2011.

[4] R. C. Mundargi, V. R. Babu, V. Rangaswamy, P. Patel, and T. M. Aminabhavi, "Nano/micro technologies for delivering macromolecular therapeutics using poly(d,l-lactide-co-glycolide) and its derivatives," *Journal of Controlled Release,* vol. 125, pp. 193-209, 2008.

[5] H. Tamberab, P. Johansenac, H. P. Merklea, and B. Gander, "Formulation aspects of biodegradable polymeric microspheres for antigen delivery," *Advanced Drug Delivery Reviews,* vol. 57, pp. 357-376, 2005.

[6] P. B. O'Donnell and J. W. McGinity, "Preparation of microspheres by the solvent evaporation technique," *Advanced Drug Delivery Reviews,* vol. 28, pp. 25-42, 1997.

[7] M. Ye, S. Kim, and K. Park, "Issues in long-term protein delivery using biodegradable microparticles," *Journal of Controlled Release,* vol. 146, pp. 241-260, 2010.

[8] T. Vermonden, R. Censi, and W. E. Hennink, "Hydrogels for Protein Delivery," *Chemical Reviews,* vol. 112, pp. 2853-2888, 2012/05/09 2012.

[9] Y. Capan, G. Jiang, S. Giovagnoli, K.-H. Na, and P. DeLuca, "Preparation and characterization of poly(D,L-lactide-co-glycolide) microspheres for controlled release of human growth hormone," *Aaps Pharmscitech,* vol. 4, pp. 147-156, 2003.

[10] T. R. H. Vitae and D. S. K. Vitae, "Hydrogels in drug delivery: Progress and challenges," *Polymer,* vol. 49, pp. 1993-2007, 2008.

[11] C.-H. Zheng, J.-Q. Gao, Y.-P. Zhang, and W.-Q. Liang, "A protein delivery system: biodegradable alginate-chitosan-poly(lactic-co-glycolic acid) composite

microspheres," *Biochemical and biophysical research communications,* vol. 323, pp. 1321-7, 2004.

[12] A. Schoubben, P. Blasi, S. Giovagnoli, L. Perioli, C. Rossi, and M. Ricci, "Novel composite microparticles for protein stabilization and delivery," *European journal of pharmaceutical sciences : official journal of the European Federation for Pharmaceutical Sciences,* vol. 36, pp. 226-34, 2009.

[13] X. L. Zheng, Y. Z. Huang, C. H. Zheng, S. Y. Dong, and W. Q. Liang, "Alginate-Chitosan-PLGA Composite Microspheres Enabling Single-Shot Hepatitis B Vaccination," *Aaps Journal,* vol. 12, pp. 519-524, Dec 2010.

[14] K. Fu, D. Pack, A. Klibanov, and R. Langer, "Visual Evidence of Acidic Environment Within Degrading Poly(lactic-co-glycolic acid) (PLGA) Microspheres," *Pharmaceutical Research,* vol. 17, pp. 100-106, 2000/01/01 2000.

[15] V. Bhardwaj and M. N. V. R. Kumar, "Drug Delivery Systems to Fight Cancer," in *Fundamentals and Applications of Controlled Release Drug Delivery*, J. Siepmann, R. A. Siegel, and M. J. Rathbone, Eds., ed: Springer US, 2012, pp. 493-516.

[16] K. Jain, "Drug Delivery Systems - An Overview," in *Drug Delivery Systems*. vol. 437, K. Jain, Ed., ed: Humana Press, 2008, pp. 1-50.

[17] J. B. Wolinsky, Y. L. Colson, and M. W. Grinstaff, "Local drug delivery strategies for cancer treatment: Gels, nanoparticles, polymeric films, rods, and wafers," *Journal of Controlled Release,* vol. 159, pp. 14-26, 4/10/ 2012.

[18] J. Tsung and D. Burgess, "Biodegradable Polymers in Drug Delivery Systems," in *Fundamentals and Applications of Controlled Release Drug Delivery*, J. Siepmann, R. A. Siegel, and M. J. Rathbone, Eds., ed: Springer US, 2012, pp. 107-123.

[19] R. Dinarvand, F. Dorkoosh, M. Hamidi, and S. H. Moghadam, "Polymeric Delivery Systems for Biopharmaceuticals," *Biotechnology and Genetic Engineering Reviews,* vol. 21, pp. 147-182, 2004/11/01 2004.

[20] Q. He and J. Shi, "Mesoporous silica nanoparticle based nano drug delivery systems: synthesis, controlled drug release and delivery, pharmacokinetics and biocompatibility," *Journal of Materials Chemistry,* vol. 21, pp. 5845-5855, 2011.

[21] D. Loca, J. Locs, K. Salma, J. Gulbis, I. Salma, and L. Berzina-Cimdina, "Porous Hydroxyapatite Bioceramic Scaffolds for Drug Delivery and Bone Regeneration," *IOP Conference Series: Materials Science and Engineering,* vol. 18, p. 192019, 2011.

[22] N. H. S. Rajeev Jain, A. Waseem Malick and Christopher T. Rhodes, "Controlled Drug Delivery by Biodegradable Poly(Ester) Devices: Different Preparative Approaches," *Drug Development and Industrial Pharmacy,* vol. 24, pp. 703-727, 1998.

[23] H. Zhou, J. G. Lawrence, and S. B. Bhaduri, "Fabrication aspects of PLA-CaP/PLGA-CaP composites for orthopedic applications: A review," *Acta Biomaterialia,* vol. 8, pp. 1999-2016, 2012.

[24] J.-M. Lü, X. Wang, C. Marin-Muller, H. Wang, P. H. Lin, Q. Yao, *et al.*, "Current advances in research and clinical applications of PLGA-based nanotechnology," *Expert Review of Molecular Diagnostics,* vol. 9, pp. 325-341, 2009/05/01 2009.

[25] A. N. Ford Versypt, D. W. Pack, and R. D. Braatz, "Mathematical modeling of drug delivery from autocatalytically degradable PLGA microspheres — A review," *Journal of Controlled Release,* vol. 165, pp. 29-37, 1/10/ 2013.

[26] S. Fredenberg, M. Wahlgren, M. Reslow, and A. Axelsson, "The mechanisms of drug release in poly(lactic-co-glycolic acid)-based drug delivery systems—A review," *International Journal of Pharmaceutics,* vol. 415, pp. 34-52, 8/30/ 2011.

[27] H. K. Makadia and S. J. Siegel, "Poly Lactic-co-Glycolic Acid (PLGA) as Biodegradable Controlled Drug Delivery Carrier," *Polymers,* vol. 3, pp. 1377-1397, 2011.

[28] X. S. Wu and N. Wang, "Synthesis, characterization, biodegradation, and drug delivery application of biodegradable lactic/glycolic acid polymers. Part II: Biodegradation," *Journal of Biomaterials Science, Polymer Edition,* vol. 12, pp. 21-34, 2001/01/01 2001.

[29] W. L. Lee, E. Widjaja, and S. C. J. Loo, "One-Step Fabrication of Triple-Layered Polymeric Microparticles with Layer Localization of Drugs as a Novel Drug-Delivery System," *Small,* vol. 6, pp. 1003-1011, 2010.

[30] Y. Yeo and K. Park, "Control of encapsulation efficiency and initial burst in polymeric microparticle systems," *Archives of pharmacal research,* vol. 27, 2004.

[31] I. Donati and S. Paoletti, "Material Properties of Alginates," in *Alginates: Biology and Applications,* H. A. R. Bernd, Ed., ed: Springer Verlag, 2009, p. 1.

[32] K. I. Draget and C. Taylor, "Chemical, physical and biological properties of alginates and their biomedical implications," *Food Hydrocolloids,* vol. 25, pp. 251-256, 2011.

[33] K. Y. Lee and D. J. Mooney, "Alginate: Properties and biomedical applications," *Progress in Polymer Science*, vol. 37, pp. 106-126, 2012.

[34] O. Smidsrød and G. Skjåk-Bræk, "Alginate as immobilization matrix for cells," *Trends in Biotechnology*, vol. 8, pp. 71–78, 1990.

[35] M. George and T. E. Abraham, "Polyionic hydrocolloids for the intestinal delivery of protein drugs: Alginate and chitosan — a review," *Journal of Controlled Release*, vol. 114, pp. 1-14, 2006.

[36] M. Sittig, "Pharmaceutical Manufacturing Encyclopedia, Volumes 1-2 (2nd Edition)," ed: William Andrew Publishing/Noyes.

[37] R. W. Pero, A. Olsson, M. Simanaitis, A. Amiri, and I. Andersen, "Pharmacokinetics, toxicity, side effects, receptor affinities and in vitro radiosensitizing effects of the novel metoclopramide formulations, sensamide and neu-sensamide," *Pharmacol Toxicol*, vol. 80, pp. 231-9, 1997.

[38] N. M. Zaki, G. A. Awad, N. D. Mortada, and S. S. Abd ElHady, "Enhanced bioavailability of metoclopramide HCl by intranasal administration of a mucoadhesive in situ gel with modulated rheological and mucociliary transport properties," *European Journal of Pharmaceutical Sciences*, vol. 32, pp. 296-307, 2007.

[39] W. Baeyens and P. De Moerloose, "Fluorescence properties of metoclopramide and its determination in pharmaceutical dosage forms," *Analyst*, vol. 103, pp. 359-367, 1978.

[40] G. O. Phillips and P. A. Williams. *Handbook of Hydrocolloids (2nd Edition)*. Available: http://app.knovel.com/hotlink/toc/id:kpHHE00002/handbook-hydrocolloids/handbook-hydrocolloids

[41] G. O. Phillips and P. A. Williams, "Handbook of Food Proteins," ed: Woodhead Publishing.

[42] T. J. Montville and K. R. Matthews, "Food Microbiology - An Introduction (2nd Edition)," ed: American Society for Microbiology (ASM).

[43] H. A. McKenzie and F. H. White Jr, "Lysozyme and α-Lactalbumin: Structure, Function, and Interrelationships," in *Advances in Protein Chemistry*. vol. Volume 41, F. M. R. J. T. E. C.B. Anfinsen and S. E. David, Eds., ed: Academic Press, 1991, pp. 173-315.

[44] J. P. Nicholson, M. R. Wolmarans, and G. R. Park, "The role of albumin in critical illness," *British Journal of Anaesthesia,* vol. 85, pp. 599-610, October 1, 2000 2000.

[45] T. Peters Jr, "Serum Albumin," in *Advances in Protein Chemistry*. vol. Volume 37, J. T. E. C.B. Anfinsen and M. R. Frederic, Eds., ed: Academic Press, 1985, pp. 161-245.

[46] Q. Yue, T. Shen, C. Wang, C. Gao, and J. Liu, "Study on the Interaction of Bovine Serum Albumin with Ceftriaxone and the Inhibition Effect of Zinc (II)," *International Journal of Spectroscopy*, vol. 2012, p. 9, 2012.

[47] T. Peters Jr, "1 - Historical Perspective," in *All About Albumin*, T. Peters, Ed., ed San Diego: Academic Press, 1995, pp. 1-8.

[48] Sigma Aldrich Product Information: Albumin from Bovine Serum. Available: http://www.sigmaaldrich.com/content/dam/sigma-aldrich/docs/Sigma/Product_Information_Sheet/b4287pis.pdf

[49] Y. Xiao and S. N. Isaacs, "Enzyme-linked immunosorbent assay (ELISA) and blocking with bovine serum albumin (BSA)—not all BSAs are alike," *Journal of Immunological Methods,* vol. 384, pp. 148-151, 10/31/ 2012.

[50] H. Towbin, T. Staehelin, and J. Gordon, "Electrophoretic transfer of proteins from polyacrylamide gels to nitrocellulose sheets: procedure and some applications," *Proceedings of the National Academy of Sciences,* vol. 76, pp. 4350-4354, September 1, 1979 1979.

[51] P. K. Smith, R. I. Krohn, G. T. Hermanson, A. K. Mallia, F. H. Gartner, M. D. Provenzano, *et al.*, "Measurement of protein using bicinchoninic acid," *Analytical Biochemistry*, vol. 150, pp. 76-85, 10// 1985.

[52] M. M. Bradford, "A rapid and sensitive method for the quantitation of microgram quantities of protein utilizing the principle of protein-dye binding," *Analytical Biochemistry*, vol. 72, pp. 248-254, 5/7/ 1976.

[53] F. Ito, H. Fujimori, and K. Makino, "Incorporation of water-soluble drugs in PLGA microspheres," *Colloids and surfaces. B, Biointerfaces,* vol. 54, pp. 173-8, 2007.

[54] F. Ito, H. Fujimori, and K. Makino, "Factors affecting the loading efficiency of water-soluble drugs in PLGA microspheres," *Colloids and surfaces. B, Biointerfaces*, vol. 61, pp. 25-9, 2008.

[55] W. L. Lee, M. Hong, E. Widjaja, and S. C. J. Loo, "Formation and Degradation of Biodegradable Triple-Layered Microparticles," *Macromolecular Rapid Communications,* vol. 31, pp. 1193-1200, 2010.

[56] M. F. Ficheux, L. Bonakdar, F. Leal-Calderon, and J. Bibette, "Some Stability Criteria for Double Emulsions," *Langmuir,* vol. 14, pp. 2702-2706, 1998/05/01 1998.

[57] T. F. Tadros, "Emulsion Science and Technology: A General Introduction," in *Emulsion Science and Technology*, ed: Wiley-VCH Verlag GmbH & Co. KGaA, 2009, pp. 1-56.

[58] J. Jiao and D. J. Burgess, "Multiple Emulsion Stability: Pressure Balance and Interfacial Film Strength," in *Multiple Emulsions*, ed: John Wiley & Sons, Inc., 2007, pp. 1-27.

[59] Y. Yeo, N. Baek, and K. Park, "Microencapsulation methods for delivery of protein drugs," *Biotechnology and Bioprocess Engineering,* vol. 6, pp. 213-230, 2001/08/01 2001.

[60] A. Taluja, Y. S. Youn, and Y. H. Bae, "Novel approaches in microparticulate PLGA delivery systems encapsulating proteins," *Journal of Materials Chemistry,* vol. 17, pp. 4002-4014, 2007.

[61] E. Widjaja, N. Crane, T.-C. Chen, M. D. Morris, M. A. Ignelzi, and B. R. McCreadie, "Band-Target Entropy Minimization (BTEM) Applied to Hyperspectral Raman Image Data," *Applied Spectroscopy,* vol. 57, pp. 1353-1362, 2003.

[62] E. Widjaja, W. L. Lee, and S. C. J. Loo, "Application of Raman Microscopy to Biodegradable Double-Walled Microspheres," *Analytical Chemistry,* vol. 82, pp. 1277-1282, 2010.

[63] M. P. A. Lim, W. L. Lee, E. Widjaja, and S. C. J. Loo, "One-step fabrication of core-shell structured alginate-PLGA/PLLA microparticles as a novel drug delivery system for water soluble drugs," *Biomaterials Science,* vol. 1, pp. 486-493, 2013.

[64] C. Sartori, D. S. Finch, B. Ralph, and K. Gilding, "Determination of the cation content of alginate thin films by FTi.r. spectroscopy," *Polymer,* vol. 38, pp. 43-51, 1997.

[65] E. Pretsch, P. Bühlmann, and M. Badertscher, "IR Spectroscopy," in *Structure Determination of Organic Compounds*, ed: Springer Berlin Heidelberg, 2009, pp. 1-67.

[66] V. Shrivastava and U. K. Jain, "Design of Single Dose Control Release Device for Antigen Delivery based on Poly (Lactic-Co-Glycolic Acid)," *International Journal of Pharmaceutical Science and Nanotechnology,* vol. 3, pp. 1075-1084, December 2010 2010.

[67] T. Florence Alexander and D. Whitehill, "Stability and Stabilization of Water-in-Oil-in-Water Multiple Emulsions," in *Macro- and Microemulsions*. vol. 272, ed: American Chemical Society, 1985, pp. 359-380.

[68] S. Magdassi and N. Garti, "Release of electrolytes in multiple emulsions: coalescence and breakdown or diffusion through oil phase?," *Colloids and Surfaces,* vol. 12, pp. 367-373, 1984.

[69] N. Garti, A. Romano-Pariente, and A. Aserin, "The effect of additives on release from w/o/w emulsions," *Colloids and Surfaces,* vol. 24, pp. 83-94, 1987.

[70] W. L. Lee, C. Loei, E. Widjaja, and S. C. J. Loo, "Altering the drug release profiles of double-layered ternary-phase microparticles," *Journal of Controlled Release,* vol. 151, pp. 229-238, 2011.

[71] T. R. Hoare and D. S. Kohane, "Hydrogels in drug delivery: Progress and challenges," *Polymer,* vol. 49, pp. 1993-2007, 2008.

[72] C. Sun, J. Yang, X. Wu, X. Huang, F. Wang, and S. Liu, "Unfolding and Refolding of Bovine Serum Albumin Induced by Cetylpyridinium Bromide," *Biophysical Journal,* vol. 88, pp. 3518-3524.

[73] G. Skjåk-Bræk, H. Grasdalen, and O. Smidsrød, "Inhomogeneous polysaccharide ionic gels," *Carbohydrate Polymers,* vol. 10, pp. 31-54, 1989.

Appendix

List of Publication related to work done in this project

- M. P. A. Lim, W. L. Lee, E. Widjaja, and S. C. J. Loo, "One-step fabrication of core-shell structured alginate-PLGA/PLLA microparticles as a novel drug delivery system for water soluble drugs," Biomaterials Science, vol. 1, pp. 486-493, 2013.

- Patent: Methods Of Manufacturing Core-Shell Microparticles, And Microparticles Formed Thereof (WO2013119183 A1; PCT/SG2013/000051)